Chapter 6

Solar Wind

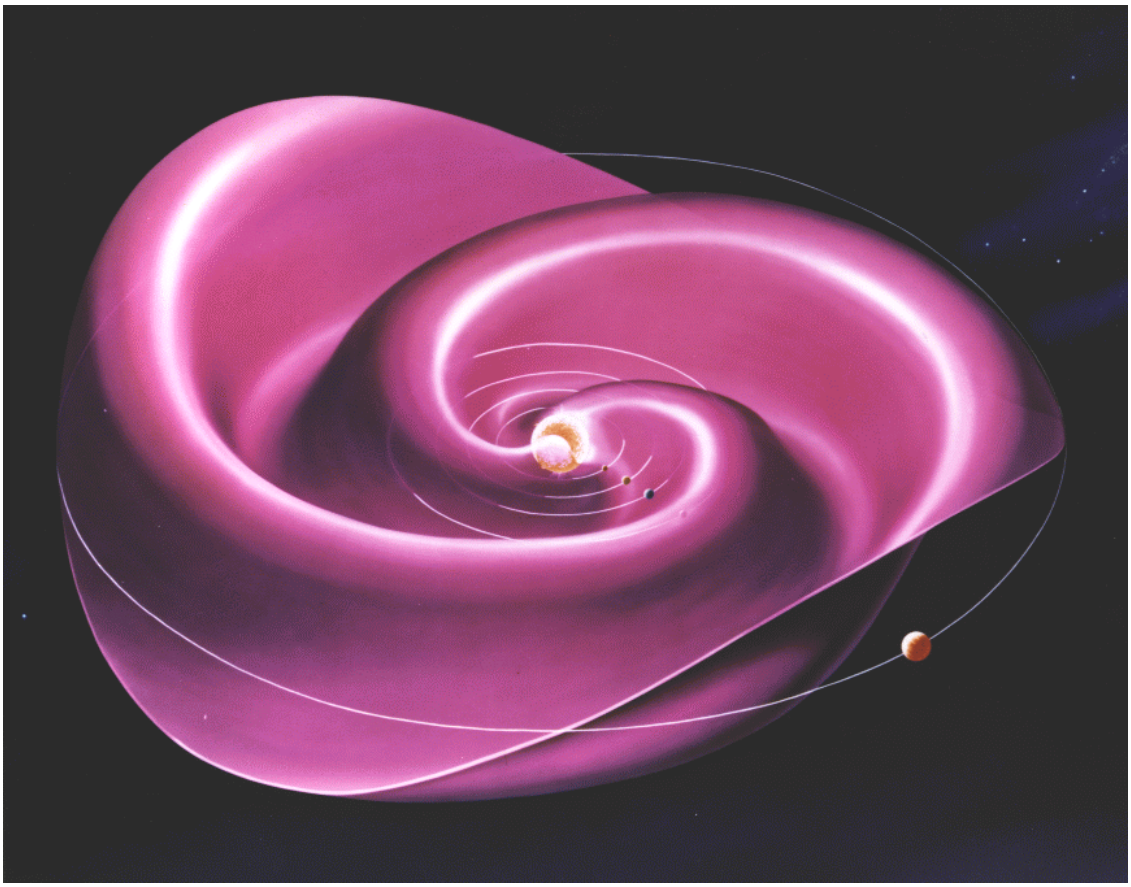

www.skywave-radio.org

Revised 11/2024

6 Solar Wind

The solar wind emanates from the Sun's inner coronal region where temperatures are over 1 million degrees Kelvin. The corona consists primarily of electrically charged electrons, protons, and helium nuclei plus a small percentage of partially ionized heavier elements such as iron. At temperatures well over 1 million degrees some of the lighter particles (electrons, protons, and helium nuclei) acquire sufficient kinetic energy to escape the Sun's gravitational pull. At speeds in excess of the Sun's escape velocity of 618 km per second these particles flow outward from the Sun into interplanetary spaces creating the solar wind. The particles gradually slow down as they travel outward so in the vicinity of Earth their speed is typically 300 to 450 km/s.

Physically the solar wind is a low density, very tenuous, highly variable, and turbulent plasma of high speed charged particles. The super high conductivity and kinetic energy of the escaping particles is considerably greater than the energy density of the Sun's coronal region magnetic field. Consequently, some of the Sun's magnetic field is "dragged away" along with the escaping particles creating a small embedded magnetic field within the solar wind. This magnetic field is often referred to as being "frozen into" the solar wind since it is a permanent part of the wind. The solar wind expands throughout the solar system carrying its magnetic field with it. For this reason, the solar wind magnetic field is called the Interplanetary Magnetic Field (IMF).

We are protected to a large extent from the solar wind by Earth's magnetic field (the magnetosphere) which diverts the solar winds past the Earth. The magnetosphere is the blue region shown in Figure 1. We now know that Mars once had rivers and lakes much like Earth. But the solar wind stripped Mars of its atmosphere and evaporated its lakes and rivers when Mars lost its protective magnetic field due to internal cooling of the planet.

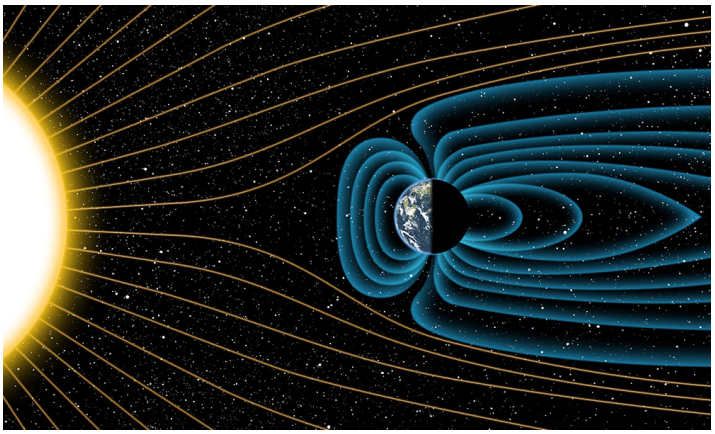

Figure 1 Earth's protective magnetosphere (blue) deflecting solar winds (yellow)
(credit: University of Rochester)

The solar wind is a considerable threat to astronauts traveling to the moon and beyond and a major consideration affecting the design of interplanetary spacecraft. The solar wind severely distorts Earth's magnetosphere creating geomagnetic storms. These storms and related events disrupt communications, including HF radio communications and GPS networks. They also have the potential of severely damaging electric power distribution systems causing wide spread long term power outages. Solar wind induced power outages have occurred in the past. The threat posed by the solar wind is so severe in our technological age that we have placed fleets of spacecraft in orbit around both the Earth and the Sun to study and monitor the solar wind and events on the Sun from which the wind originates. This activity has resulted in the creation of a new scientific and engineering field known as Space Weather. The organizations involved in Space Weather are charged with the responsibility of providing accurate predictions of solar wind conditions and electromagnetic radiation from the Sun to power grid managers, airlines with flights near the north polar region, and others, in addition to satellite and space flight mission control operators. Accurate space weather predictions allow operations personnel to place their systems in protective modes or change routes when solar wind conditions warrant.

6.1 History

Throughout history there have been hints that events on the Sun affected the Earth. Chinese observers were aware of sunspots more than 2,000 years ago. Observation of sunspots became fairly common in Europe beginning in the seventeenth century. Of particular interest was the absence of sunspots from 1645 to 1710, a period known as the Maunder minimum. Some believed the lack of sunspots to be the cause of unusually cold weather that Europe experienced at the time (the little ice age), although today that view is questioned.

Studies of Earth's geomagnetic field from the 1850's on seemed to indicate that Earth's magnetic field was some how being affected by events occurring on the Sun. In the early twentieth century it was fairly well established that solar flares and other activity on the Sun did in fact perturb Earth's magnetic field. These disruptions were (and are) called geomagnetic storms. It was also discovered that activity on the Sun affected the intensity of galactic cosmic rays arriving at Earth from their origins deep within interstellar space. The change in cosmic ray intensity was found to often be quite abrupt with return to normal levels occurring slowly. The implication being that whatever was emanating outward from the Sun was disrupting the incoming flux of cosmic rays far beyond Earth's orbit. Thus, the long time delay required for cosmic rays to return to normal levels. It was further discovered that cosmic ray intensity decreased at solar maximum and returned to "normal" levels during solar minimum.

Theories as to why these phenomena occurred began to emerge by mid twentieth century. In the early 1950's L. Biermann suggested that a continuous plasma outflow from the Sun, a solar wind which varied in intensity with solar activity, could account for disruptions in Earth's magnetic field. The strongest evidence that some type of solar wind existed came from the study of comets. As the comet shown in Figure 2 loops around the Sun, its tail always points away from the Sun suggesting that some type of solar out flow was pushing the tail away from the Sun. Interestingly a comet actually has two tails. A tail consisting of dust particles that bends back toward the comet's orbit

and a second tail consisting of electrically charged ions that stretches out radially from the Sun as shown in Figure 2.

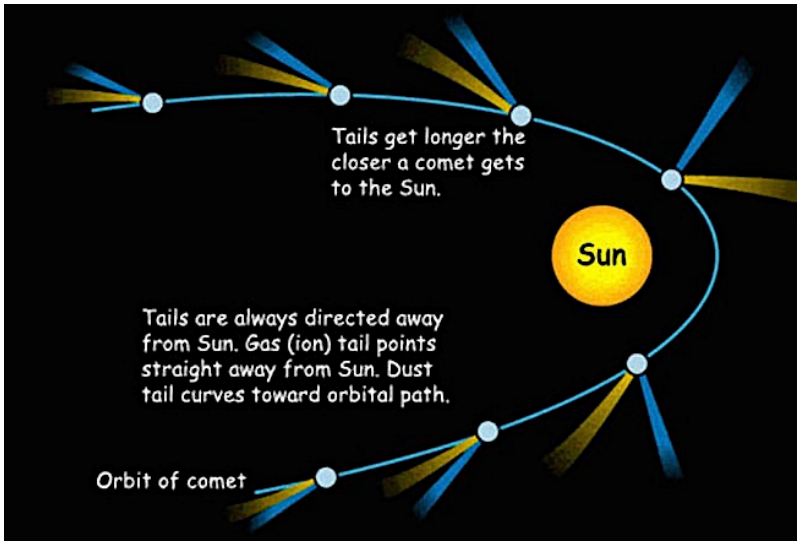

Figure 2 Comet Tails (source: universetoday.com)

In 1957 S. Chapman developed a model showing that the corona's high thermal conductivity and hot plasma could result in the corona expanding far out from the Sun's photosphere. Influenced by the work of Biermann and Chapman, Eugene Parker developed a hydrodynamical model in 1958 for a continuously expanding corona, or supersonic solar wind, that extends well past the Earth and other planets of the solar system. The Mariner 2 Venus probe in 1962 and the Voyager 1 and 2 spacecraft launched in 1977 provided early confirmation of Parker's once controversial theory.

Over the past 60 years measurements from numerous spacecraft traveling throughout the solar system have confirmed the presence of a solar wind flowing outward from the Sun past all of the planets and into interstellar space. These spacecraft include the Parker Solar Probe approaching to within 0.04 AU (Astronomical Units) of the Sun (Figures 3) and the Voyager 1 spacecraft over 152 AU from the Sun (Figure 4). One Astronomical Unit is the distance from the Sun to the Earth (92.9 million miles or 149.6 million km). Voyagers 1 and 2 have both left the solar system and are now in interstellar space (see voyager.jpl.nasa.gov Mission Status).

It is important to note that the solar wind and IMF can not be observed from Earth's surface because of Earth's protective geomagnetic field illustrated in Figure 1. Consequently, we did not have verification of the theorized solar wind or knowledge of the embedded IMF until we began launching spacecraft to Venus and the other planets in the 1960s and 1970s.

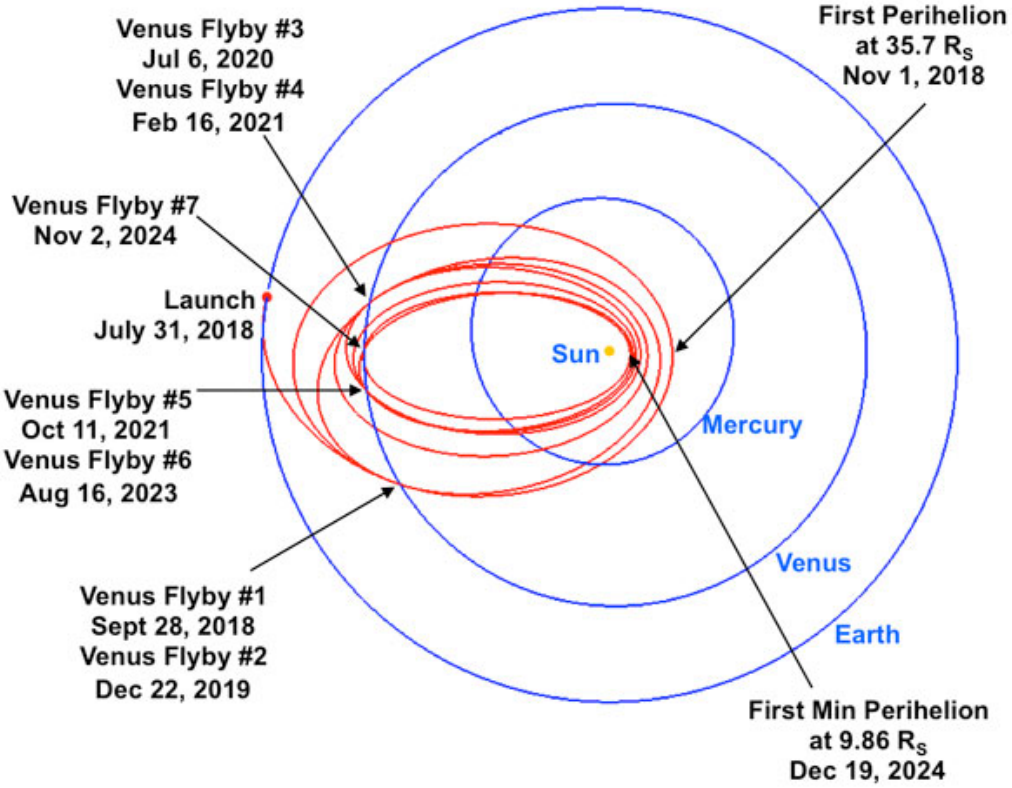

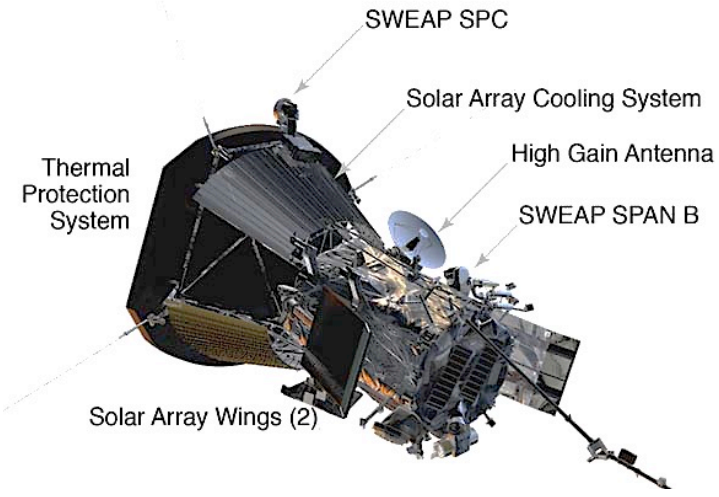

Figure 3 Parker Solar Probe (source: University of Alabama – Huntsville)

Notice the very elliptical orbit of the Parker Solar Probe. It swings in close to the Sun, approaching to within 35.7 to 9.86 solar radii (R_S), and then travels back out past Venus before beginning another pass in close to the Sun. Notice also the "stocky" build of the spacecraft and the large thermal protective shield designed to protect it from intense solar heat on close approaches to the Sun.

In comparison, the Voyager spacecraft is "spindly" with instrumentation sticking out in multiple directions from its main body. There is no need for a compact streamlined design in the voids of outer space to which it is traveling. The most prominent aspect of the spacecraft is its large 3.7 meter high gain antenna needed to communicate back to Earth from beyond the solar system. Even so NASA's Deep Space Network of giant radio antennas positioned around the world are needed to receive Voyager's extremely weak radio signals.

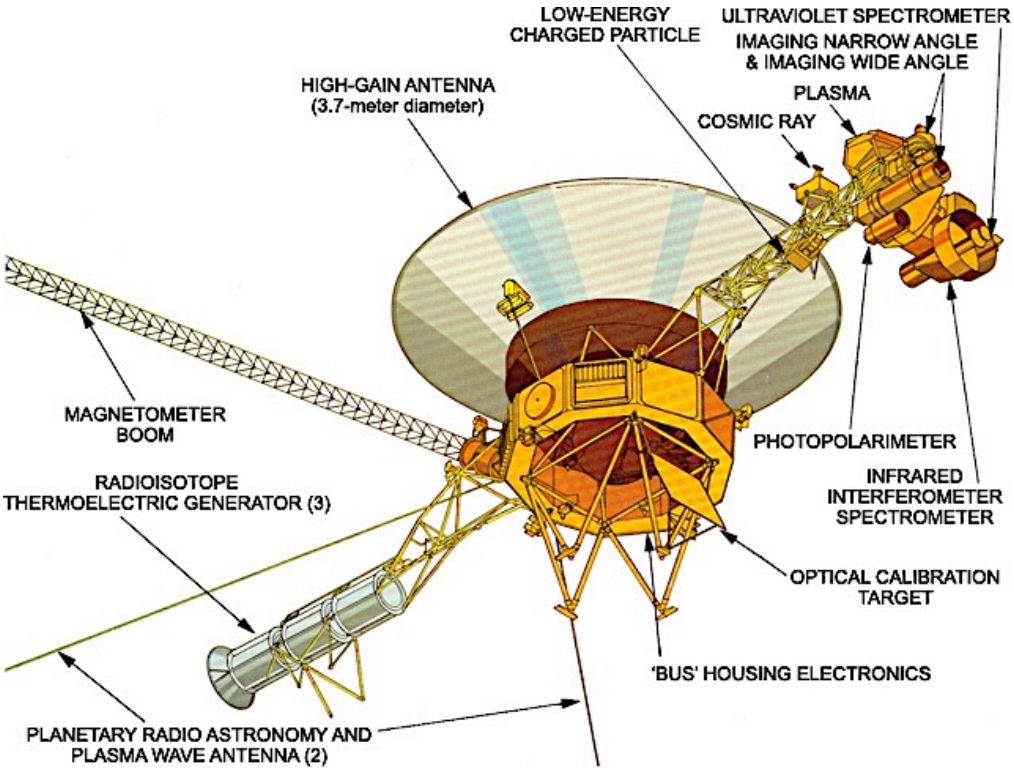

Figure 4 Voyager Spacecraft (source: NASA/JPL – Caltech)

6.2 Earth – Sun Coordinate Systems

Several different coordinate systems are used in studying the relationship between the Sun and Earth. The two most commonly used in the study of solar winds are the Geocentric Solar Magnetospheric (GSM) and Geocentric Solar Ecliptic (GSE) coordinate systems.

6.2.1 Geocentric Solar Ecliptic (GSE) System

The GSE system is the easiest to visualize. The coordinate system is centered on the Earth (geocentric) and defined relative to the solar ecliptic plane in which Earth's orbit is located. Figure 5 shows the coordinate system when the center of the Earth is located at point P. The radial x-axis (X_{GSE}) points from the center of the Earth to the center of the Sun. The y-axis (Y_{GSE}) is in the ecliptic plane tangent to Earth's orbit. The z-axis (Z_{GSE}) is perpendicular to the ecliptic plane at point P. The GSE system is widely used as the system for representing vector quantities in space physics.

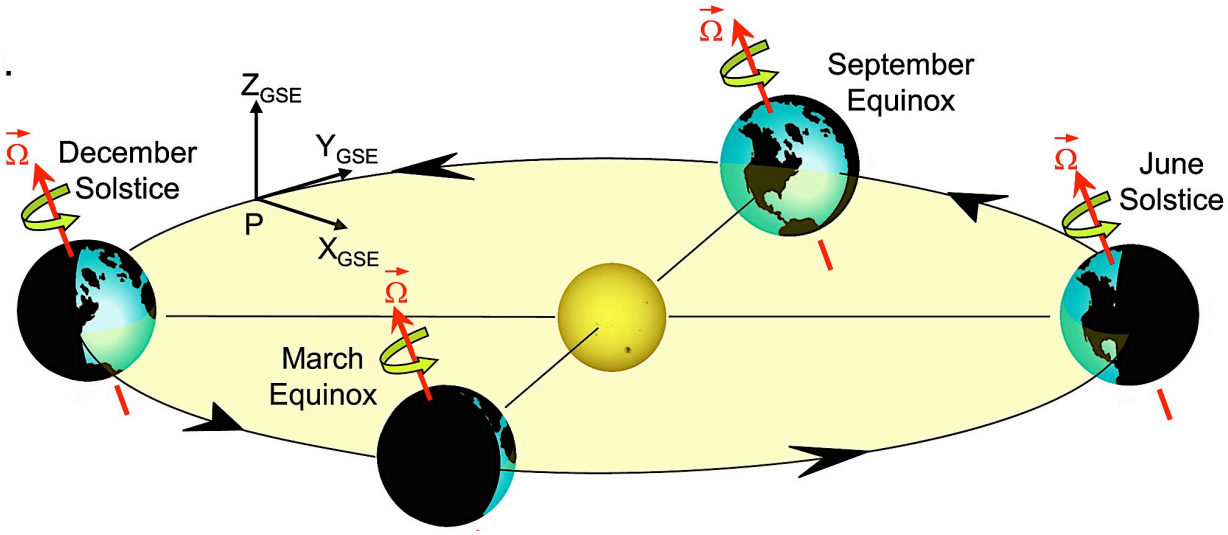

Figure 5 Geocentric Solar Ecliptic (GSE) Coordinates (source: AGU Publications)

6.2.2 Geocentric Solar Magnetospheric (GSM) Coordinate System

The GSM coordinate system, also centered on the Earth (geocentric), is defined relative to Earth's magnetic field axis as illustrated in Figure 6. The radial x-axis (X_{GSM}) points from the center of the Earth to the center of the Sun, the same as in the GSE system. However, in the GSM coordinate system the z-axis (Z_{GSM}) is aligned with Earth's magnetic field axis. The y-axis (Y_{GSM}) is perpendicular to both the x and z axis. The GSM system is considered the best system to use when studying the effects of the solar wind IMF on Earth's magnetosphere and ionosphere. Specifically, geomagnetic storms on Earth are most intense when the IMF is oriented southward in the negative Z_{GMS} direction.

The difference between the GSM and GSE systems is simply a rotation about the x-axis. In the GSE system the z-axis is perpendicular to the ecliptic plane. In the GSM system the coordinate system is rotated about the x-axis so that the z-axis is in line with the axis of Earth's magnetic field.

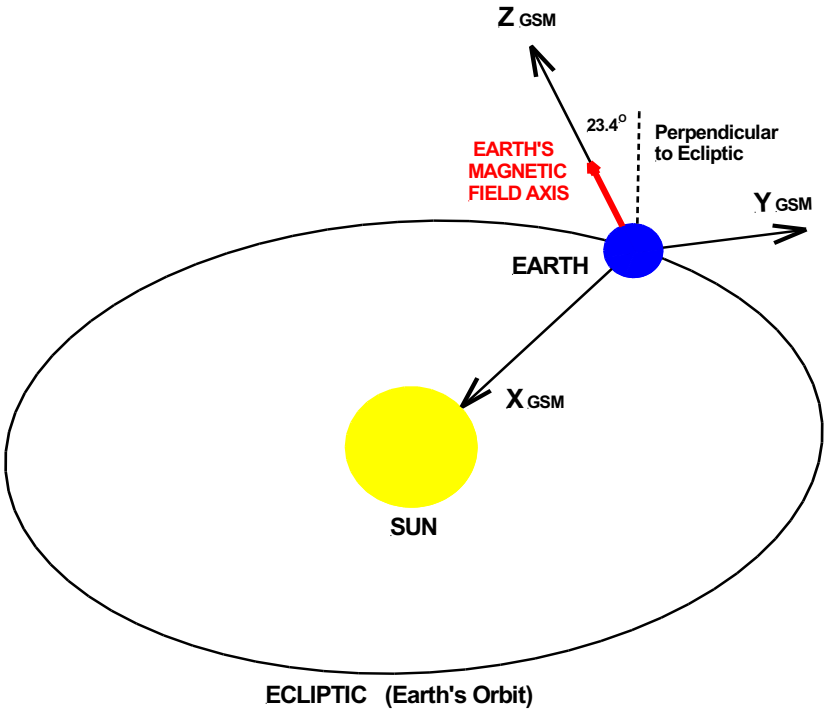

Figure 6 Geocentric Solar Magnetospheric (GSM) Coordinates (source: author)

6.3 Solar Wind Characteristics

95% of the solar wind consists of protons and electrons with the rest consisting almost entirely of doubly ionized helium nuclei (α *particles*). The density of the solar wind drops off by a factor of $1/r^2$ where r is the distance from the Sun. The plasma density in the vicinity of the Earth (at 1 AU) is on average about 5 particles per cm^3. In contrast the plasma density of Earth's ionospheric F layer is about 10^6 particles per cm^3. Thus, the solar wind is very tenuous despite its ability to do a great deal of damage.

6.3.1 Solar Wind Temperature

The temperature of the solar wind electron and proton plasma ranges from around 100,000 to 150,000 °K in the vicinity of Earth. This compares to the roughly 5,000 °K for the Sun's photosphere and over 1 million degree K for that part of the corona near the Sun. The solar wind α *particles* are about 4 to 5 times hotter.

6.3.2 Solar Wind Speed

The velocity of the solar wind in the vicinity of Earth ranges from about 250 to 750 km/s. Variations in solar wind speed are shown in Figure 7. The speed of the solar wind is between 300 to 450 km/s most of the time. This is the ambient slow speed wind emanating from the Sun on a pretty much continuous basis. The speed of the solar wind trails off rather quickly from 450 to 750 km/s. Solar winds in the range of 500 to 750 km/s are defined as high-speed winds. Notice that the high-speed winds occur infrequently compared to the nearly continuous slow speed winds. At any given time, the speed of the solar wind is about the same throughout the solar system from Earth, well past Neptune, to the outer edge of the solar system (the Heliopause) at about 100 AU.

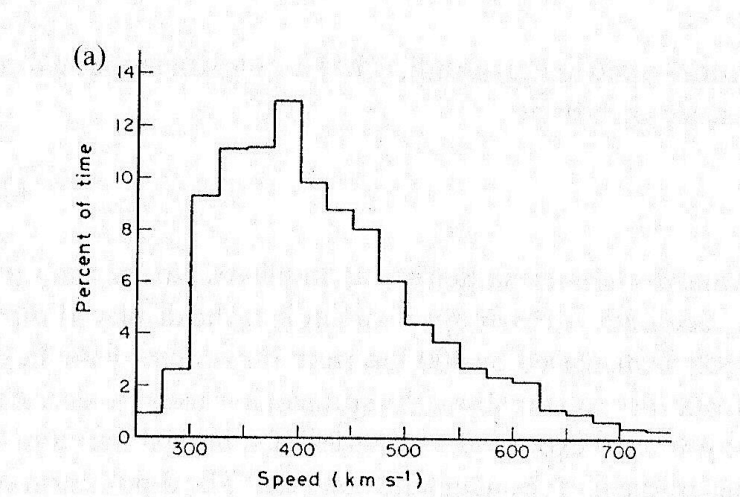

Figure 7 Solar Wind Speed (source: Hunsucker & Hargreaves)

The solar wind is supersonic as it flows past the Earth in the sense that its speed v_{sw} is greater than the speed of sound v_s through the solar wind plasma. It is also greater than the Alfven speed

$$v_{Asw} = \frac{B}{\sqrt{\mu_0 m_p n_{sw}}}$$

where

v_{Asw} = Alfven speed

B = solar wind magnetic field strength

μ_0 = permeability of free space

m_p = proton mass (in comparison, the mass of electrons is insignificant)

n_{sw} = solar wind proton number density

The speed of sound is important because it is the speed at which pressure waves propagate through the solar wind plasma. The Alfven speed is important because it is the velocity at which electrical current systems propagate through the plasma. The supersonic speed of the solar wind "out runs" the speed of pressure waves and electrical currents propagating in the solar wind plasma.

6.3.3 Interplanetary Magnetic Field

As introduced earlier, the solar wind's weak embedded magnetic field is known as the Interplanetary Magnetic Field (IMF). The magnetic field originates internal to the Sun. However, in the corona a small portion of the Sun's magnetic field becomes "frozen in" the solar wind plasma due to the plasma's very high electrical conductivity. The kinetic energy of the solar wind plasma is about eight times the energy density of the frozen in magnetic field. Consequently, the motion of the total solar wind magneto-plasma is governed by the motion of the plasma particles rather than by its magnetic field.

The strength of the IMF field varies between 0 to about 25 nT as shown in Figure 8. Its average strength is about 5.6 nT. In comparison, Earth's magnetic field strength at Earth's surface is 30,500 nT. The unit of magnetic field strength is the Tesla where 1 Tesla = 10,000 Gauss while 1 nT = 10^{-9} T = 10^{-5} G. The strength of the IMF drops off by a factor of 1/r where r is again the distance from the Sun.

The strengths of the B_Z and B_Y components of the IMF are also shown in Figure 8 where B_Z and B_Y are the z and y axis components of the magnetic field in the Geocentric Solar Magnetosphere (GSM) coordinate system (Figure 6). B_Z is the north – south component of the magnetic field and B_Y is the east – west component.

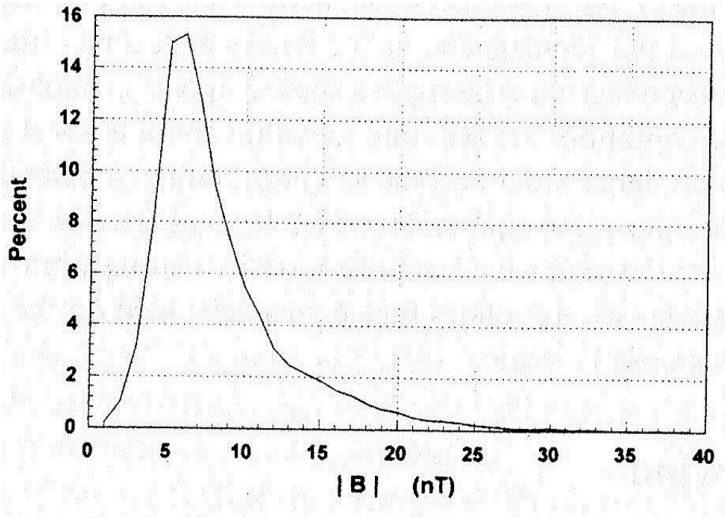

Variation in the magnitude of the IMF field |B|

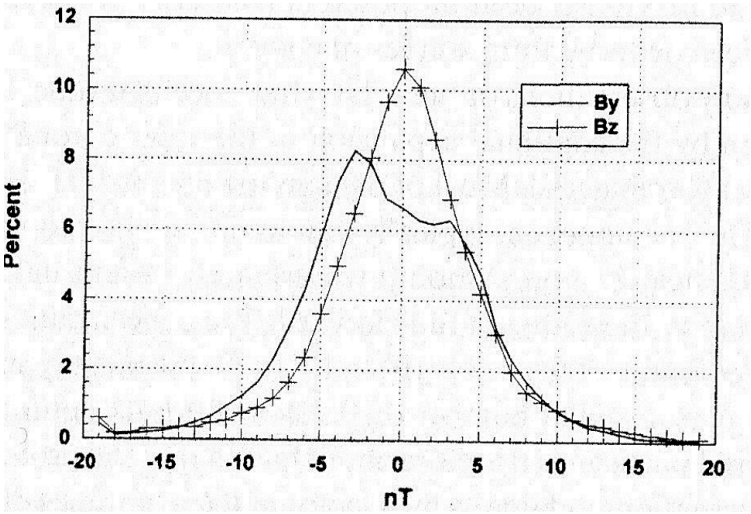

Figure 8 Interplanetary Magnetic Field Strength (source: Hunsucker & Hargreaves)

The important north - south B_Z component of the field is zero most of the time (10% of the time). It is directed southward (- B_Z) about the same amount of time as it is pointed northward. This is important because southward directed fields tend to create geomagnetic storms while northward directed fields do not.

The IMF is in a radial direction near the Sun. That is, the B_X component is predominate while B_Y is essentially zero. However, the Sun's rotation bends the IMF into an Archimedes spiral pattern as illustrated in Figure 9. This spiral shape is generally referred to as a Parker-spiral in honor of astrophysicist Eugene Parker who in the mid 1950s developed the theory of supersonic solar winds and predicted their shape as they propagate away from the Sun. The Parker-spiral is very much like a rotating lawn sprinkler. The jets of water form a spiral pattern when viewed from above even though the trajectory of the individual water droplets is radially outward from the sprinkler. At Earth's orbit the direction of the IMF field lines in the ecliptic plane are about 45° with respect to the radial direction. Consequently, near Earth radial B_X and east-west B_Y components of the IMF are about equal in magnitude. At the orbits of Jupiter and Saturn the IMF field lines are at an angle of nearly 90° with respect to the radial direction from the Sun (B_Y is dominate and B_X is essentially zero). However, it should be noted that the direction of the magnetic field fluctuates widely from these time averaged directions.

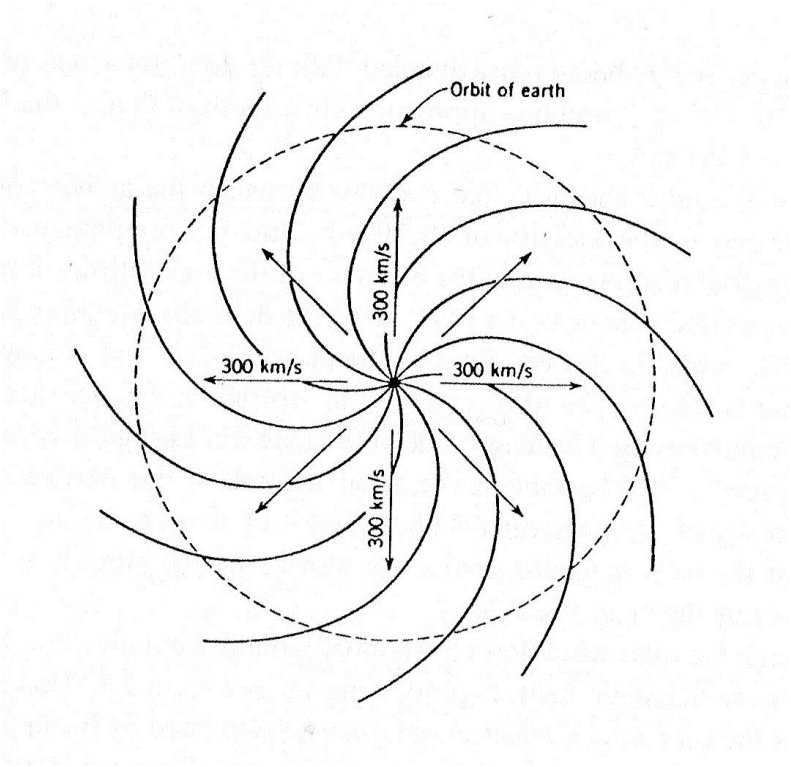

Figure 9 Parker-Spiral Shape of Solar Wind and IMF (source: Hunsucker & Hargreaves)

6.4 Solar Wind Sector Structure

One of the most significant aspects of the IMF is the changes in the polarity of the field's radial component near the ecliptic plane. The radial component B_X can abruptly switch from outward away from the Sun (+ direction) to inward toward the Sun (- direction) as the IMF sweeps past Earth. These changes often occur several times during the Sun's 27 days rotational period. The polarity reversals create a solar wind sector structure as view from the Earth. This structure is illustrated in Figure 10.

Four sectors are shown in Figure 10. This is not always the case. The number of sectors typically vary from 2 to 4. In addition, the sectors are not necessarily the same size. In Figure 10 one of the sectors is smaller than the other three. In addition, the density and speed of the solar wind can change from one sector to another. Density can vary by a factor of ten while the solar wind speed can change by a factor of 2.

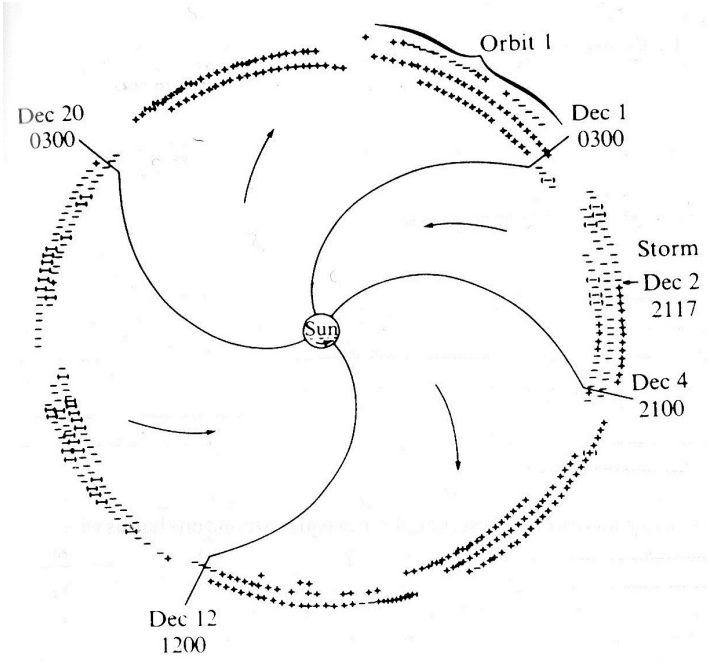

Figure 10 IMF Sector Structure (source: Hunsucker & Hargreaves)

The reason for the apparent sector structure is shown in Figure 11. On a large scale, the Sun's magnetic field is essentially bipolar with its magnetic poles M tilted with respect to its rotational axis Ω . Most of the magnetic field lines are closed in that they begin and terminate on the Sun's surface (they have two foot points on the Sun). The remaining magnetic field lines are open extending far out into interplanetary space without ever returning to the Sun. These magnetic field lines only have a single foot point on the Sun.

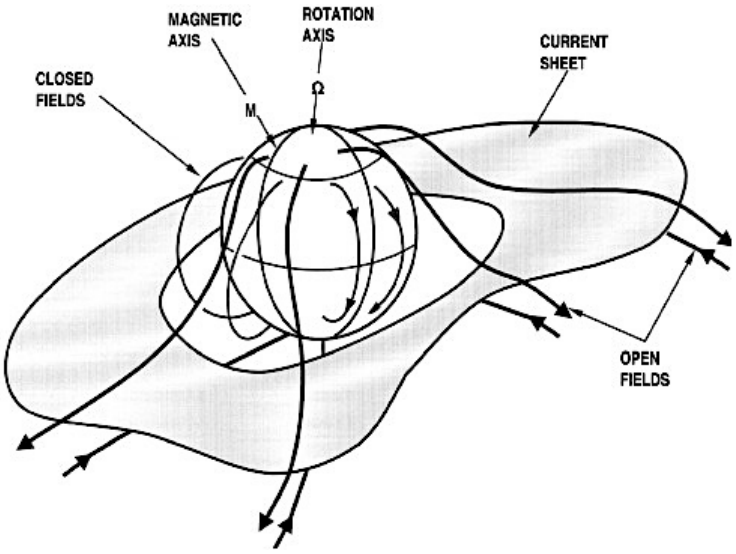

Figure 11 Solar Magnetic Field and Current Sheet (source: ScienceDirect.com)

The open magnetic field lines in the northern hemisphere of the Sun flow outward away from the Sun. These field lines are defined to be in a positive or + direction. In the southern hemisphere open field lines flow inward toward the Sun (in a negative or – direction). Near the ecliptic plane the oppositely directed open field lines are separated by a thin current sheet known as the Heliospheric Current Sheet (HCS). Like the magnetic field itself, the current sheet is also tilted with respect to the Sun's rotational axis and ecliptic plane. Consequently, as the Sun rotates a spacecraft near the Earth could, for example, observer the outward magnetic field from the Sun's northern hemisphere. Later, as the tilted current sheet sweeps by, the spacecraft would see the magnetic field abruptly change direction to that of the Sun's southern hemisphere inward directed magnetic field. Consequently, to a spacecraft located on the ecliptic plane, the rotating magnetic field appears to have two sectors. A spacecraft situated high above the ecliptic plane and the titled current sheet would see only a single sector, a continuous positive magnetic field flowing out from the Sun's northern hemisphere or a negative field flowing into the southern hemisphere.

Additional sectors may appear to an observer on the ecliptic plane, 4 sectors for example, because the current sheet is not flat but tends to be warped and undulate up and down creating folds much like the skirt of a pirouetting ballerina. For this reason, Figure 11 is known as the ballerina model. Figure 12 shows a three dimensional representation of the current sheet.

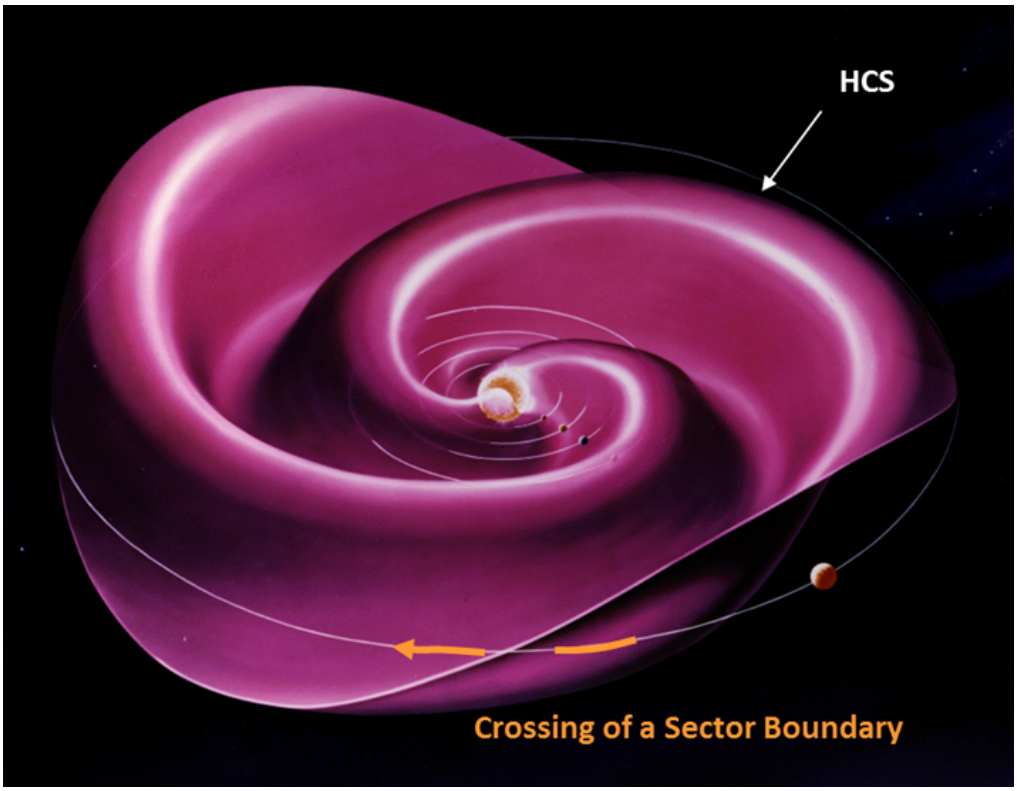

Figure 12 Three – Dimensional Representation of the Heliospheric Current Sheet
(source: Solar - Terrestrial Centre of Excellence)

A change in the solar wind radial (X_{GSM}) magnetic field orientation occurs when the Earth traverses a fold as illustrated in Figure 12. This is called a Sector Boundary Crossing (SBC). The change in orientation can be quite abrupt from outward (+ direction ~ 180^o) to inward (- direction ~ 0^o relative to the X_{GSM} axis) or visa versa. The orientation angle is known as the phi angle. The phi angle is between 90^o and 270^o when the magnetic field is pointing outward away from the Sun. The angle is between 271^o and 89^o when the field is pointed inward.

A sector boundary crossing frequently causes variations in several solar wind parameters. In particular, the average magnetic field intensity can rise quickly, peak about 1 day after the crossing, and then decay. The solar wind speed typically rises to a peak on days 1-2 and then it too decays. In addition, the solar wind density often peaks around day one, falls to a minimum in the center of the sector, and then rises again toward the end of the sector. Finally, geomagnetic activity on Earth tends to increase on days 1-2 and then decays gradually through the rest of the sector.

Figure 13 shows the solar wind parameters during a Sector Boundary Crossing occurring on July 28, 2014. Notice that the phi angle (blue trace) abruptly switches from outward away from the Sun (~ 180^o) to inward (~ 360^o). On July 31 the magnetic field abruptly switches back to outward.

However, only small changes, “blips” occur in the other solar wind parameters (temperature – green trace, speed – yellow trace, and density – orange trace) during the July 28th SBC. The changes are even less dramatic during the July 31st SBC. This is often the case. Large disturbances in the geomagnetic field are usually not associated with SBCs.

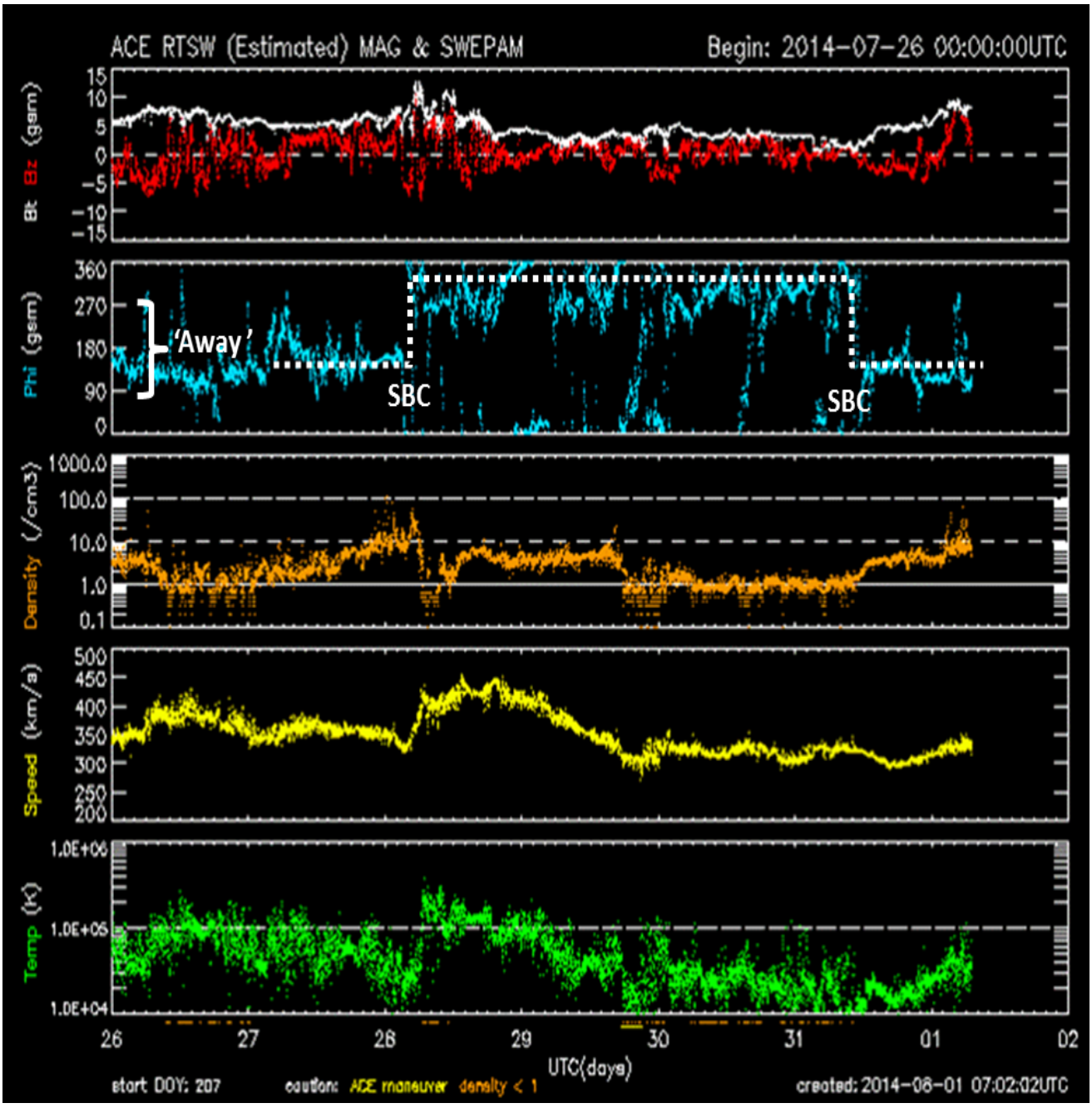

Figure 13 Solar Wind and IMF Parameters July 26 to August 1, 2015
(source: Solar - Terrestrial Centre of Excellence)

6.5 Current Solar Wind Conditions

The current solar wind conditions can be obtained from the website www.skywave-radio.org by clicking on Current Conditions and then on the Solar Wind tab. The solar wind conditions for February 2, 2021 are shown in Figure 14.

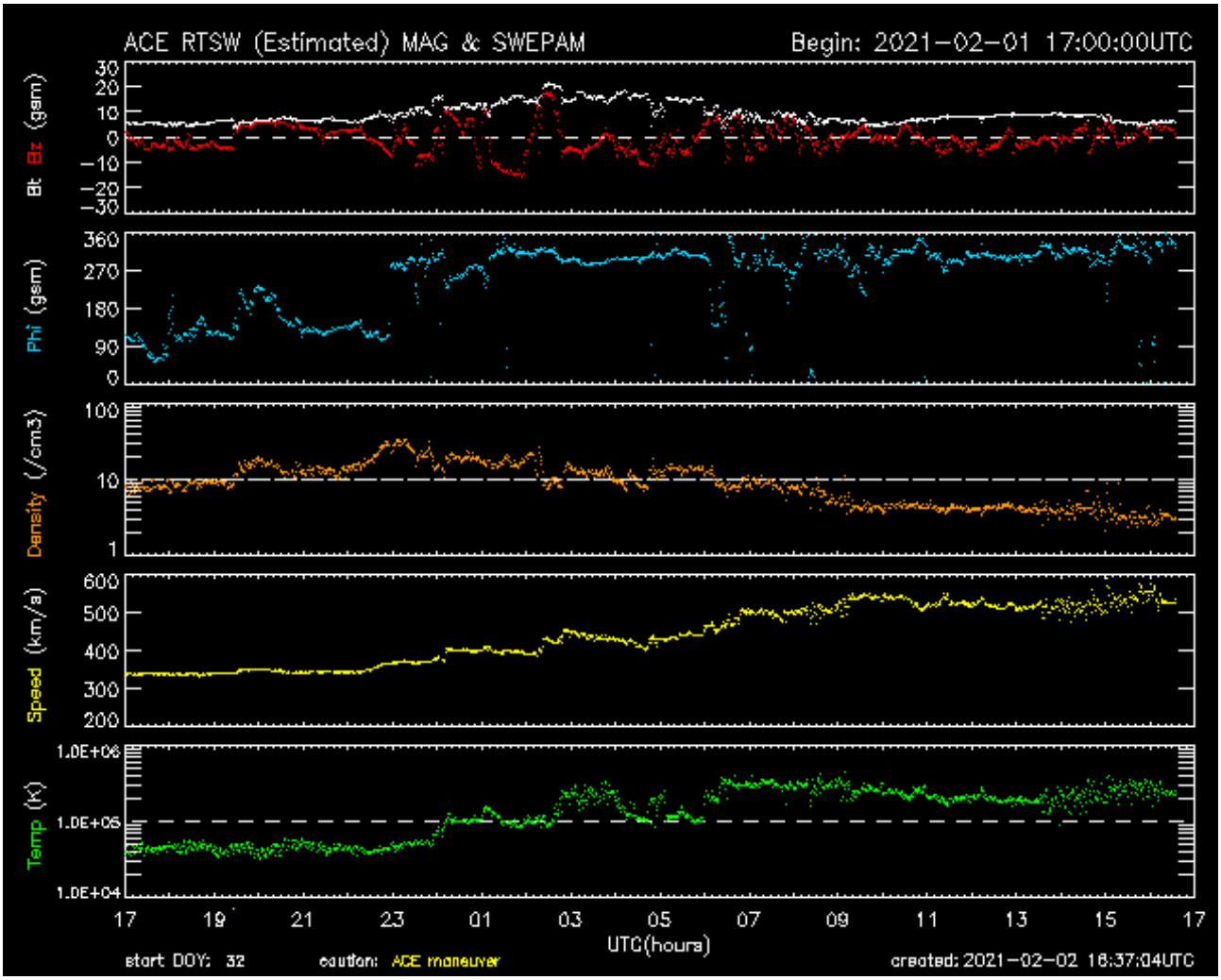

Figure 14 Solar Wind Conditions for 2/2/2021 (source Space Weather Prediction Center)

The conditions displayed are:

- **Magnetic field strength Bz of the solar wind (red trace).** The Geocentric Solar Magnetospheric coordinate system (GSM), shown in Figure 6 above, is used for the B_Z plot. A positive Bz value corresponds to a northward direct magnetic field while a southward orientated field has a negative Bz value. A southward direct field often produces strong magnetic storms on Earth.

- **Magnetic field orientation (Phi angle – blue trace)**. The phi angle is between 90° and 270° when the magnetic field is pointing outward away from the Sun and between 271° and 89° when the field is pointed inward.

- **Solar wind density per cubic centimeter (orange trace)**.

- **Solar wind speed km/s (yellow trace)**.

- **Solar wind temperature °K (green trace)**. The temperature ranges from 10,000 °K to 1,000,000 °K with the typical value being around 100,000 °K.

6.6 The Corona

The solar winds originate in the corona where temperatures are over 1 million degrees Kelvin.

The corona is situated just above the chromosphere (Figure 15). The visible white light hallo of the corona extends out more than 2 million km from the Sun. There is no actual upper boundary for the corona. It continuously thins as it stretches outward from the Sun, through the solar system, and eventually disappears into interstellar space.

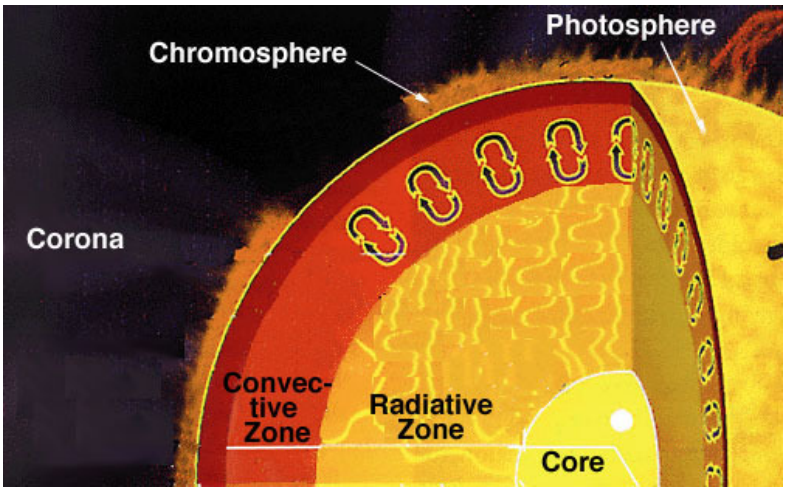

Figure 15 Structure of the Sun (source: freeburgkm.worldpress.com)

Like the chromosphere, the corona is normally not visible because the photosphere is so bright. In perspective, the photosphere is a million times brighter than the corona. During a full eclipse the white coronal light is visible surrounding the Sun as shown in Figure 16.

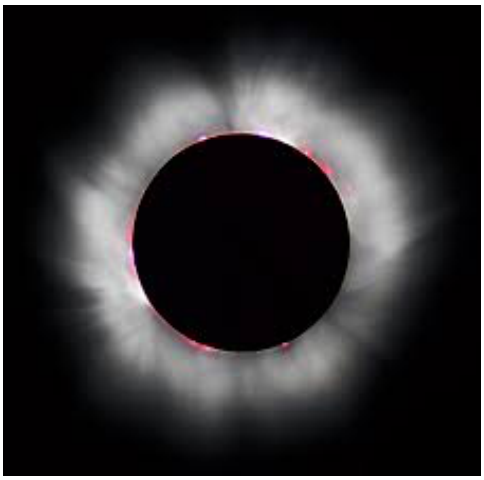

Figure 16 Solar Corona (source: Wikipedia)

The corona's white light, at altitudes out to $1.5\ x\ 10^6$ km, is produced by highly energetic free electrons scattering light radiated by the photosphere. Further out grains of interplanetary dust are responsible for the scattering.

Figure 17 shows the corona symmetrically elongated about the equator at solar minimum. During solar minimum active regions of the Sun are found at low latitudes causing the symmetrical elongation. In Figure 18 long streamers radiate outward ringing the corona during solar maximum. These streamers are driven by active regions located at higher latitudes on the Sun.

Figure 17 Corona during solar minimum (credit: NOAA)

Figure 18 Corona during solar maximum (credit: skyandtelescope.org)

Large-scale structures occurring in the corona include coronal holes (Figure 19) and helmet streamers (Figure 20).

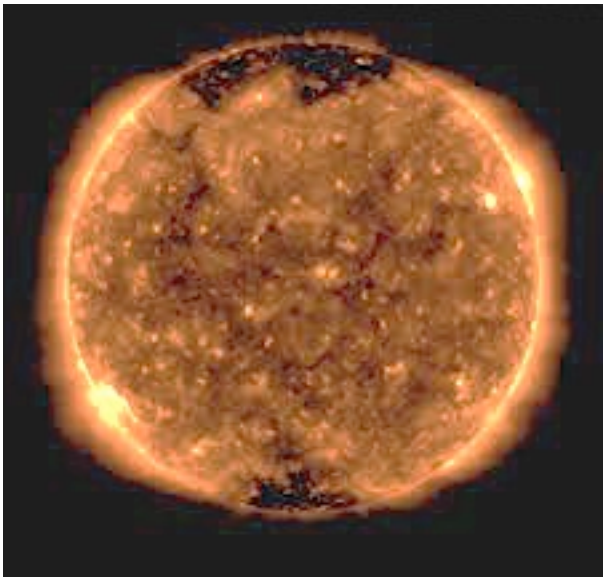

Figure 19 Large dark regions are coronal holes (credit: NOAA www.swpc.noaa.gov/phenomena)

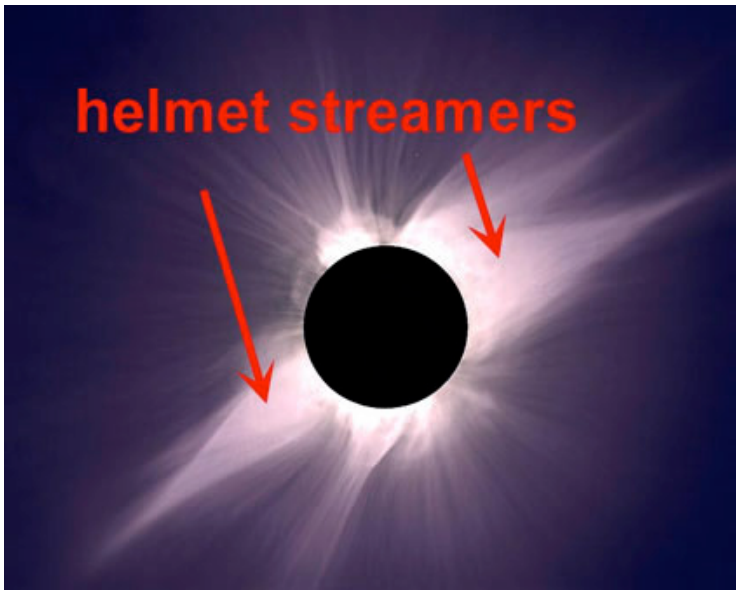

Figure 20 Helmet Streamers (source: Earth and Space Science)

During solar minimum coronal holes are typically found in the polar regions of the Sun while streamers are concentrated near the solar equatorial plane in a region known as the streamer belt.

When solar activity increases, polar coronal holes shrink and the streamer belt widens. Additional streamers, called pseudostreamers, also begin appearing at high solar latitudes outside the streamer belt. At solar maximum the Sun may be ringed by streamers as illustrated in Figure 21.

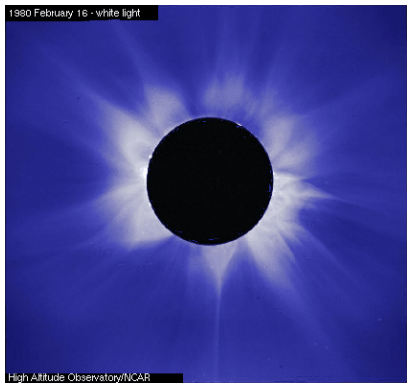

Figure 21 Streamers at Solar Maximum (source: Wikimedia commons)

A more detailed diagram of the corona illustrating coronal holes and helmet streamers is shown in Figure 22.

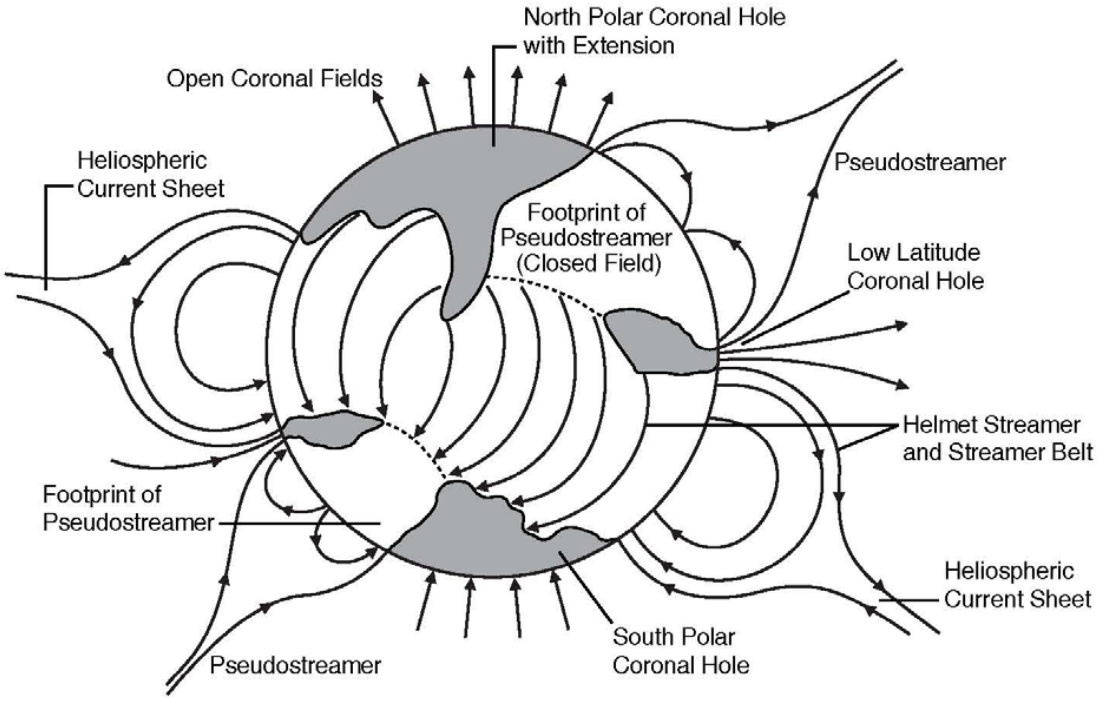

Figure 22 Structure of the Corona (source: Luhmann, Univ. of Calf. Berkeley)

6.6.1 Coronal Holes

Coronal holes are dark areas seen in the corona when viewed in Extreme Ultra Violate (EUV) and soft X-ray light. They appear dark, like those shown in Figures 19 and 22, because they are cooler and less dense than the surrounding corona plasma.

Coronal holes can develop at any time and any location on the Sun. However, they occur most often at the solar north and south poles. Some of these grow and expand into the lower solar latitudes as illustrated in Figure 22. Coronal holes can also develop in other regions of the Sun independent of the polar holes. In Figure 22 two small coronal holes are shown near the equatorial region. In some cases, independent holes split off from polar holes. Coronal holes occur most often and last longer during solar minimums. In some cases, coronal holes can last for several solar rotations, a solar rotation being about 27 days.

As illustrated in Figure 22, open magnetic field lines flow out of northern coronal holes and extend far out into interplanetary space while open magnetic field lines flow into southern coronal holes.

Coronal holes are the source of high-speed solar winds which flow outward way from the Sun along the open coronal hole magnetic field lines. The high-speed winds typically reach speeds of 500 to 750 km/s (over 1 million miles per hour). High speed winds can reach the Earth in as little as 40 hours.

6.6.2 Solar Prominences, Coronal Loops and Coronal Streamers

Figures 23 and 24 illustrate solar prominences, coronal loops and coronal streamers. Figure 23 clearly shows the positions and depths of the Photosphere, Chromosphere, Transition Region, and the Corona, as well as numerous looping structures. Figure 24 identifies the small loops on the left side of the figure as prominences that extend from the Photosphere into the Chromosphere and Transition Region. The much larger loops in the center are coronal loops that extend into the Corona far above the Photosphere and Chromosphere. A coronal streamer is shown on the right with its characteristic pointed top. These loops are formed by closed magnetic fields erupting from the Sun's surface with each loop having two-foot points anchored in the Photosphere. Figure 24 also illustrates the difference between closed and open magnetic fields.

It would appear that the three types of loops are pretty much the same with coronal loops simply being larger. However, the characteristics of prominences and coronal loops are quite different.

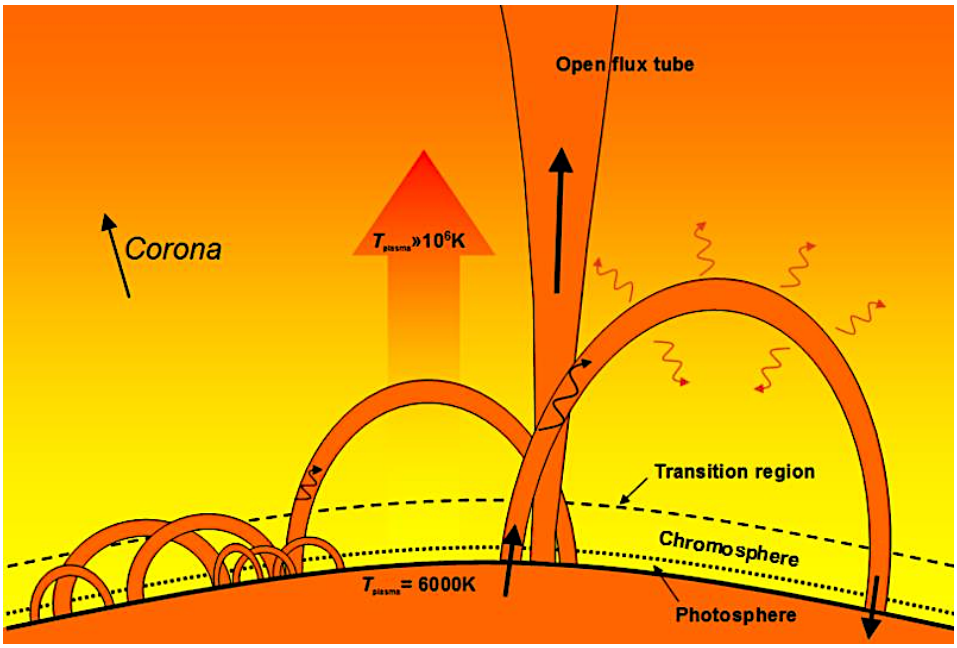

Figure 23 Prominences and Corona Loops (source: eclipse2017.nasa.gov/solar-prominences)

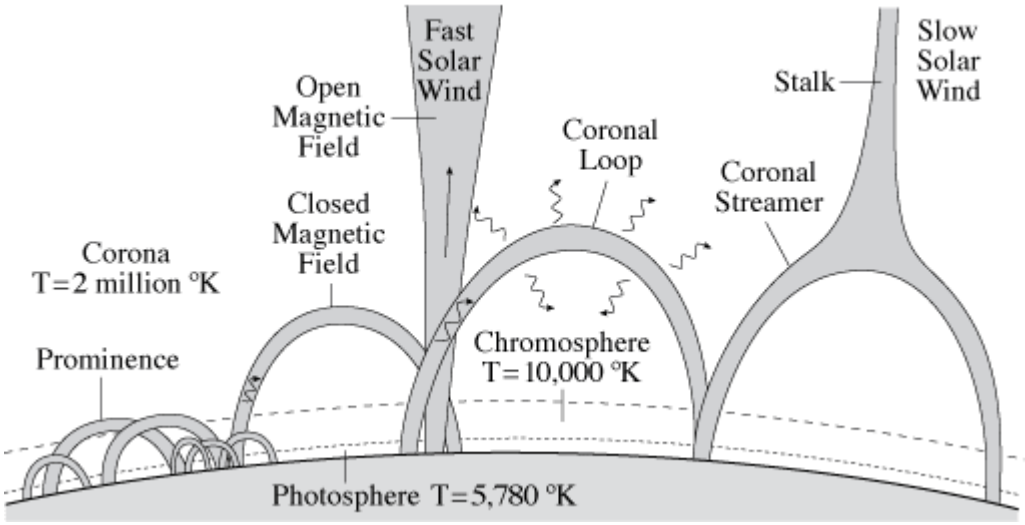

Figure 24 Prominences, Loops & Streamers (source: NASA's Marshall Space Flight Center)

6.6.2.1 Prominences

Prominences are large bright loops and curtains of relatively cool plasma suspended above the photosphere by strong arching magnetic fields. Prominences are often but not always associated with sunspot regions. A prominence occurring on the edge of the Sun is shown in Figure 25.

A prominence is formed by closed arching magnetic fields erupting through the Sun's surface with the two footpoints of the arch anchored in the photosphere. The magnetic fields inside a prominence are not smooth but are instead twisted and tangled by the turbulent and convective motion of the plasma at the base of the prominence.

The erupting magnetic fields carry with them electrically charged plasma of ionized gas and neutral hydrogen atoms. The charged plasma, often traveling at speeds of 40 km/sec, follow the magnetic field contours giving prominences their arching shape. Neutral hydrogen atoms are dragged along embedded in the plasma. Hydrogen atoms emit light in the Hα spectrum, as their single electrons jumps between valence states, giving a prominence its bright reddish appearance. The strength of the magnetic field within a prominence typically ranges from 10 to 800 gauss, compared to the Sun's quiet bipolar field of around 1 gauss and intensities of over 3,000 gauss in twisted and knotted magnetic field lines. Temperature within a prominence is on the order of 7,000 degrees kelvin, much cooler and denser than the surrounding chromosphere and corona. A prominence typically has a plasma density of around 10^9 to 10^{11} particles per cm^3. Prominences usually extend through the chromosphere into the lower part of the corona and often lasts for several hours. In some cases a prominence can remain in place for 2 - 3 solar rotations, again each rotation being about 27 days. The stability of a prominence is due to the equilibrium between its opposing magnetic and gravitational forces. Disruption of this equilibrium causes prominences to collapse, sometimes catastrophically producing solar flares and coronal mass ejections.

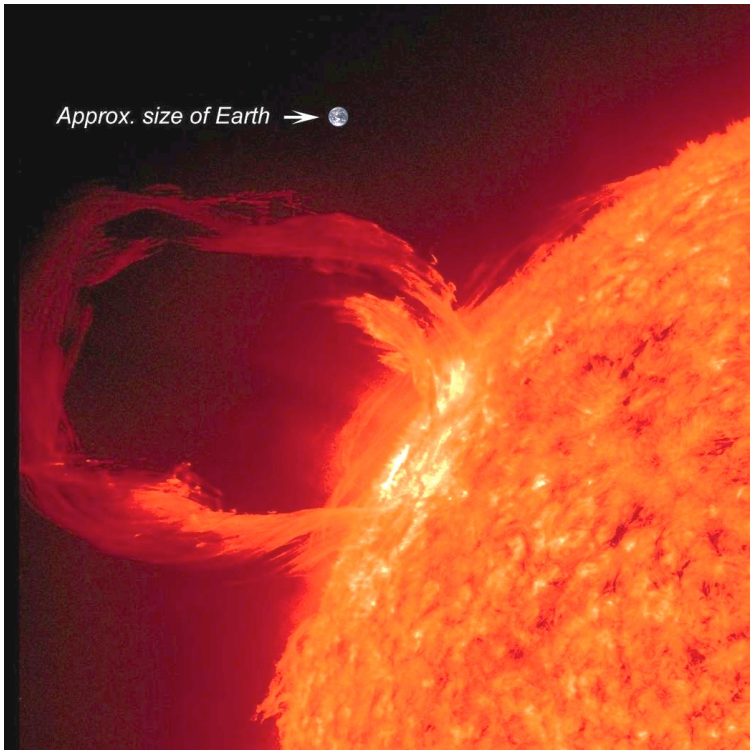

Figure 25 Active Region Eruptive Solar Prominences (credit: NASA)

Filaments and prominences are the same thing seen from different perspectives. A prominence appears as a high bright arching formation when viewed on the edge of the Sun against the black background of interplanetary space. When viewed on the face of the Sun, it appears as a dark erratic scare or filament, as illustrated in Figure 26. A filament is dark in appearance because it is relatively cool compared to the chromosphere below it.

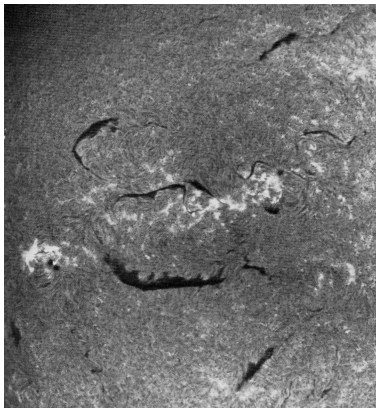

Figure 26 Filaments on the solar disk in H – alpha light. (credit: Big Bear Solar Observatory)

Prominences appear in various shapes and sizes. Prominences occurring in active regions of the Sun include eruptive prominences, like the one shown in Figure 25, spray prominences shown in Figure 27 that often precede a solar flare, and loop prominences that typically form after a flare. In active regions prominence material is often observed condensing and falling back toward the photosphere forming falling prominences like the one shown in Figure 27. Falling prominences are sometimes referred to as coronal rain.

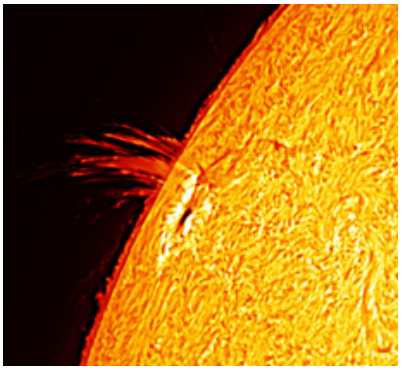

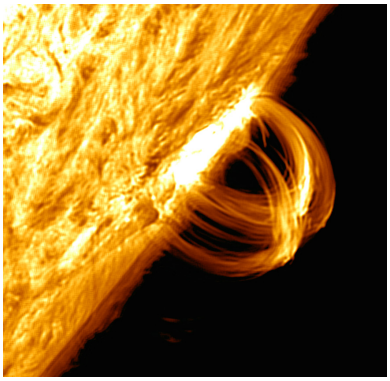

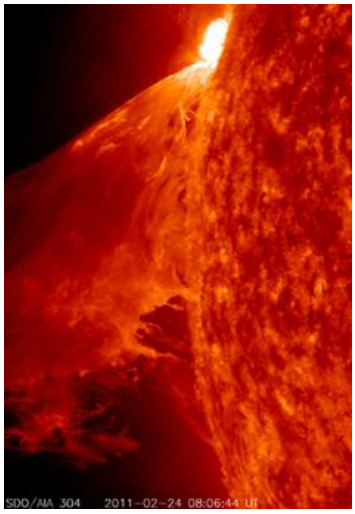

Figure 27 Spray Prominence Post Flare Loop Prominence Falling Prominences

Quiescent prominences are important because they typically are found far from active regions of the Sun. The hedgerow prominence shown in Figure 28 is a common quiescent prominence.

Figure 28 Quiescent hedgerow prominence (Source: Sky & Telescope)

6.6.2.2 Coronal Loops

Coronal loops are markedly different from prominences. Coronal loops are created by upwelling magnetic fields generated inside the Sun with their footpoints anchored in the photosphere, similar to prominences. But unlike prominences, coronal loops extend far out into the corona, as illustrated in Figures 29.

These closed magnetic structures often form above sunspot groups in active regions of the Sun. They magnetically connect one region on the solar surface to another.

Magnetic field lines within coronal loops are smoother than in prominences.

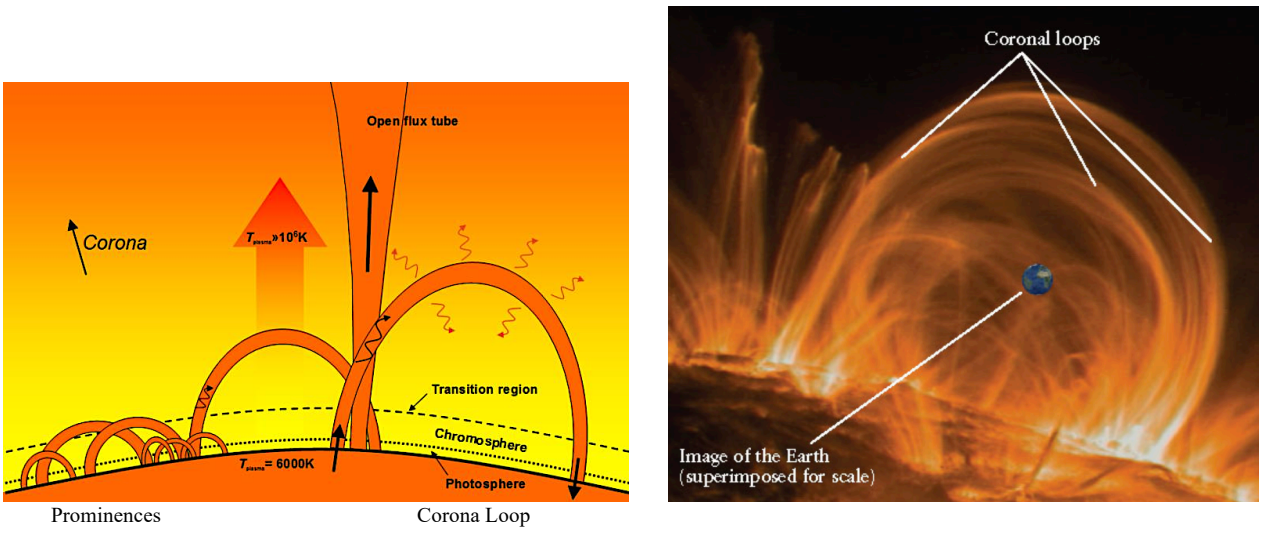

Figure 29 Corona Loops (source: eclipse2017.nasa.gov/solar-prominences)

The average plasma density of a coronal loop is about 100 particles per cm^3. In contrast, the plasma density in a prominence is on the order of 10^9 to 10^{11} particles per cm^3. Coronal loops are thus very thin and tenuous compared to prominences.

Plasma temperatures are much higher in coronal loops. The plasma temperature is over 100,000 ^oK, much hotter than the 7,000 ^oK plasma temperature in a prominence. At these high temperatures hydrogen atoms are all fully ionized, which means that each atom has lost its electron leaving behind only the atom's single proton nucleus. A nucleus can not emit light. Light is only emitted by the electrons of an atom as they jump between valance states. Consequently, unlike prominences, the light emitted by coronal loops does not come from its hydrogen atoms. Instead, the radiated light is the result of thermal emissions from its extremely hot plasma. The very hot plasma causes coronal loops to emit copious amounts of extreme ultraviolet and x-ray radiation. Some heavier ions in the plasma, such as ionized iron, still have a remaining complement of electrons that can emit

light at discrete wavelengths. These emission lines are often used to determine the exact temperature and density of coronal loop plasma.

Coronal loops do not remain static in time. Driven by motion in the underlying photosphere and convection zone, coronal loops grow in size, twist and turn, and often catastrophically collapse as their magnetic field lines become tangled and twisted.

6.6.2.3 Helmet Streamers

A coronal helmet streamer, illustrated on the right in Figure 30, is a large coronal loop that has been pinched together into an elongated point at its top by slow speed solar winds emanating from regions around the streamer. With its pointed top, called a stalk, a helmet streamer resembles a 19th century German military helmet as illustrated in Figure 30.

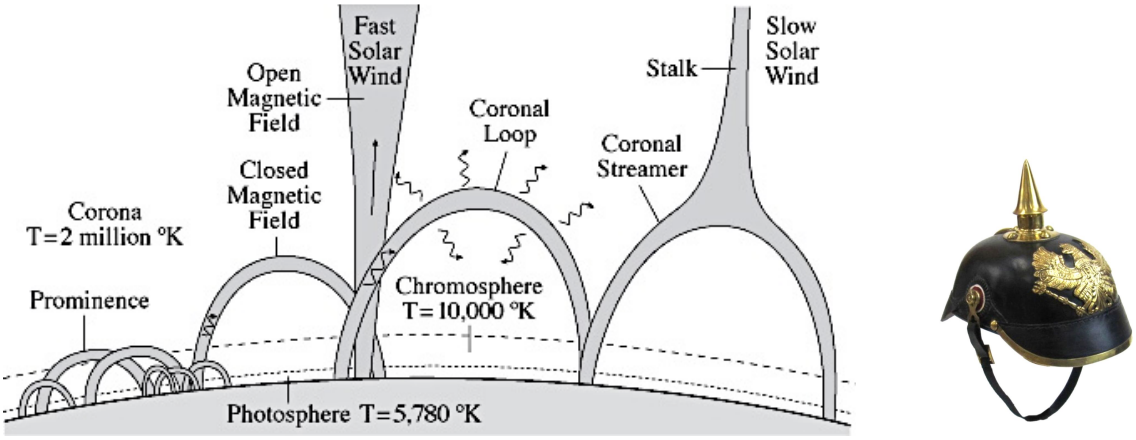

Figure 30 Coronal Helmet Streamer (source: NASA's Marshall Space Flight Center)

Helmet streamers usually overlie sunspots and prominences in the active streamer belt region of the Sun near the solar equator. A streamer is characterized by its bulb shaped base and elongated stalk extending outward from the top of the steamer. Two helmet streamers are shown in Figure 31 on the rim of the Sun. The warped heliospheric current sheet (Figure 32) runs through the middle of the streamer belt bisecting the belt and the two helmet streamers shown in Figure 31. Two pseudostreamers are also shown in the diagram, one in the upper right and the other in the lower left part of the diagram. These pseudostreamers exist outside the streamer belt and often appear during solar maximum when steamers ring the Sun as shown in Figure 21. The significant difference between helmet and pseudostreamers is that pseudostreamers are located far from the heliospheric current sheet while the current sheet cuts through helmet streamers.

Streamers are the Sun's outermost closed magnetic fields.

Slow speed solar winds with speeds of 300 – 450 km/s originate in the streamer belt region. These winds take about 140 hours to traverse the distance between the Sun and Earth. They are believed to emanate from spaces between streamers.

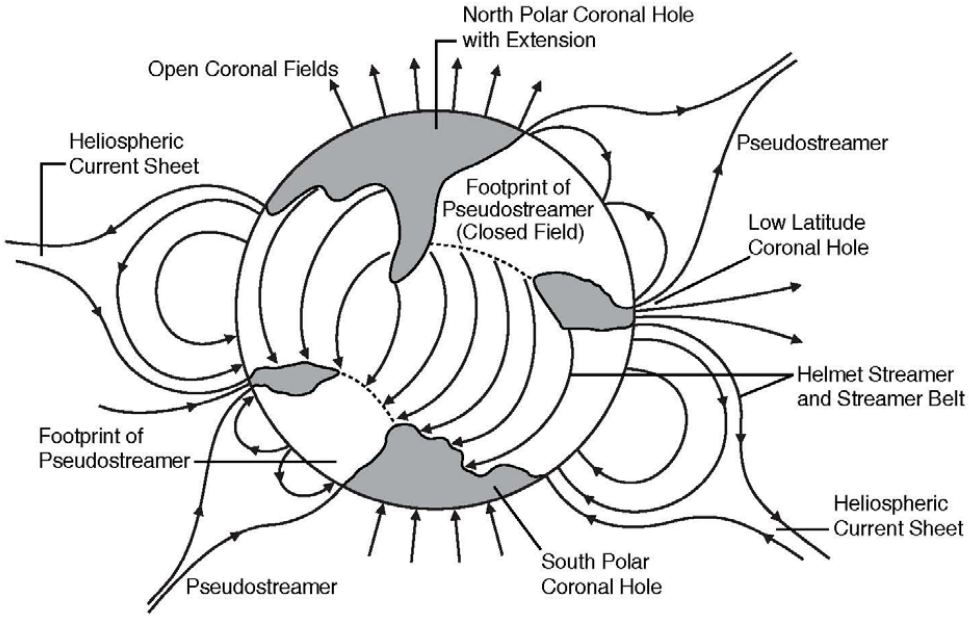

Figure 31 Structure of the Corona (source: Luhmann, Univ. of Calf. Berkeley)

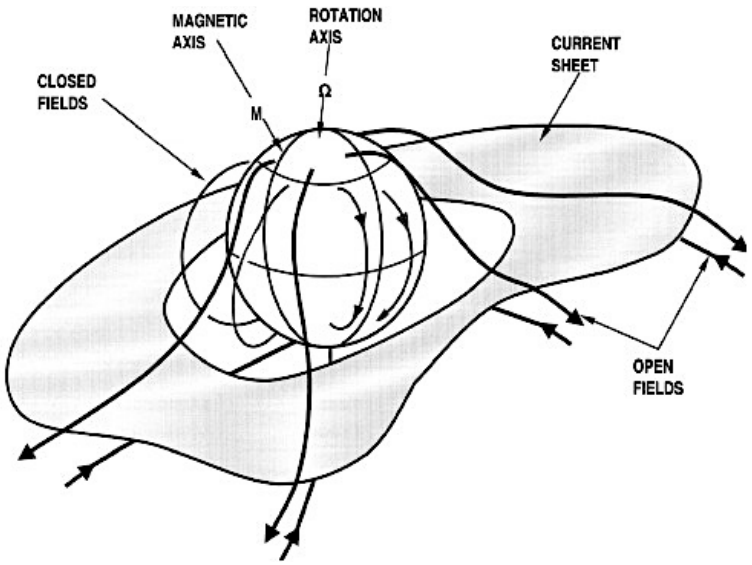

Figure 32 Solar Magnetic Field and Heliospheric Current Sheet (source: ScienceDirect.com)

6.7 Various Types of Solar Winds

There are four distinct types of solar winds originating from different regions of the Sun:

1. Streamer belt winds,
2. Coronal hole winds,
3. Sector reversal region winds, and
4. Coronal Mass Ejection (CME) winds.

The origin of the first three types of winds is shown in Figure 33.

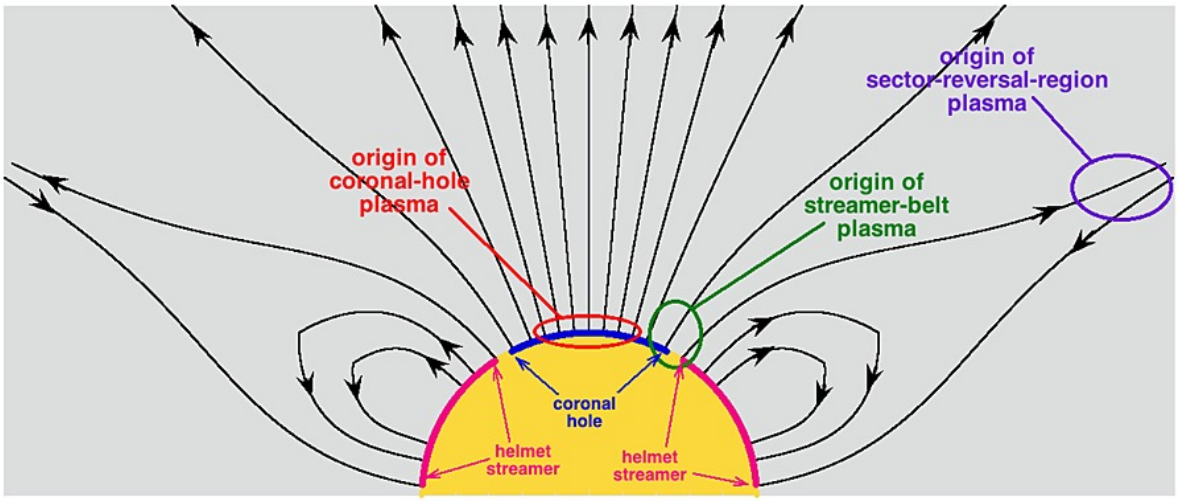

Figure 33 Source of Various Types of Solar Winds (source: Xu & Borovsky)

The average characteristics of these winds are summarized in Table 1, Figures 34 and 35.

	Streamer Belt Wind	Coronal Hole Wind	Sector Reversal Region Wind	CME (Ejecta) Wind
Wind Speed	410 km/s	562 km/s	339 km/s	429 km/s
Number Density	5.6 particles/cm^3	3.2 particles/cm^3	10.7 particles/cm^3	6.4 particles/cm^3
Field Strength	5.3 nT	5.8 nT	4.3 nT	10.6 nT
Homogeneity	Quasi-homogeneous	Quasi-homogeneous	Lumpy - plasma	Inhomogeneous
Field Orientation	Parker spiral aligned	Parker spiral aligned	Non-Parker spiral aligned	Non-Parker spiral aligned
Hours to Earth	103 h	76 h	124 h	101 h
Occurrence Rate	41.6 %	23.9 %	23.9 %	11.5 %

Table 1 Summary of Solar Wind Characteristics (averages for the years 1995 – 2018)

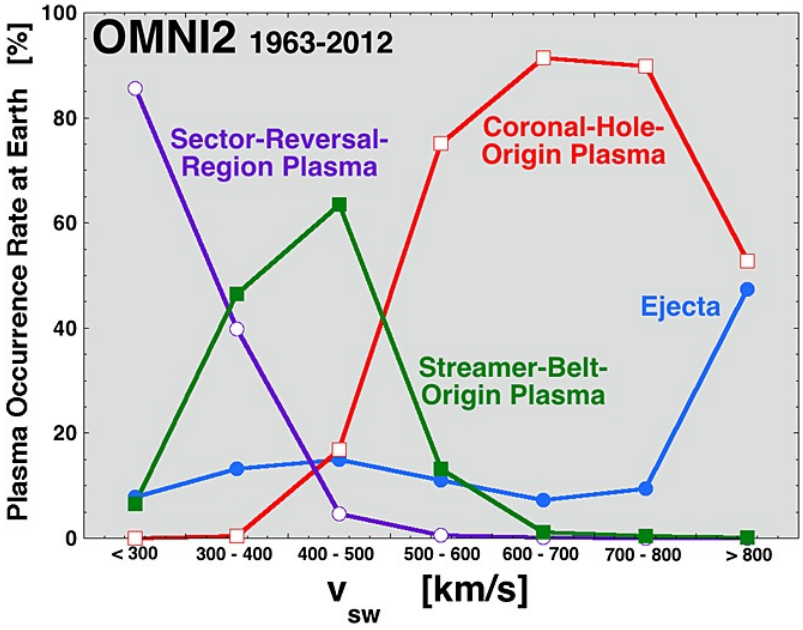

Figure 34 Solar Winds Speeds (source: Xu & Borovsky)

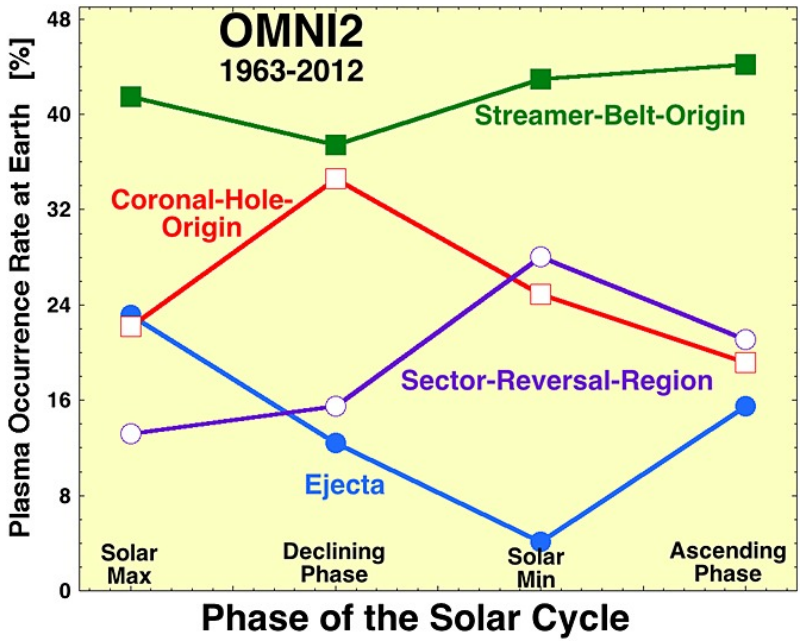

Figure 35 Occurrence of Solar Winds Throughout the solar cycle (source: Xu & Borovsky)

6.7.1 Streamer Belt Winds

The slow speed streamer belt winds are the ambient background solar winds that are continuously emanating from the Sun. For the years from 1995 through 2018 streamer belt winds accounted for 41.6 % of the solar winds reaching Earth (Figure 35). Interestingly, the 11 year solar cycle has little effect on streamer belt winds.

Streamer belt winds are believed to originate in the space between helmet streamers and from the edges of coronal holes, although their exact point of origin is still being investigated. Streamer belt winds are classified as slow solar winds with speeds typically ranging from 300 to 450 km/s (Figure 34). Streamer belt winds have the second lowest density of the four types of winds with a density of 5.6 particles per cm^3. They also have the second lowest magnetic field strength at 5.3 nT. The magnetic field orientation of streamer belt winds tends to be Parker-spiral aligned (in the same direction as the Parker-spiral shown in Figure 36) with large fluctuations about the Parker-spiral direction. Streamer belt winds also tend to be somewhat homogeneous in their composition.

Figure 36 shows the direction of the interplanetary magnetic field (IMF) as it spirals out from the Sun in the shape of the Parker-spiral. The dashed circles in Figure 36 are the orbits of selected planets. The inner most circle is the orbit of Mercury while the heavy dashed circle is the orbit of Earth. The orbit beyond Earth is that of Mars. The orbit furthest from the Sun in Figure 36 is Jupiter. Notice that the IMF cuts across Earth's orbit at nearly a 45° angle. At Jupiter the direction of the IMF is nearly in-line with Jupiter's orbit.

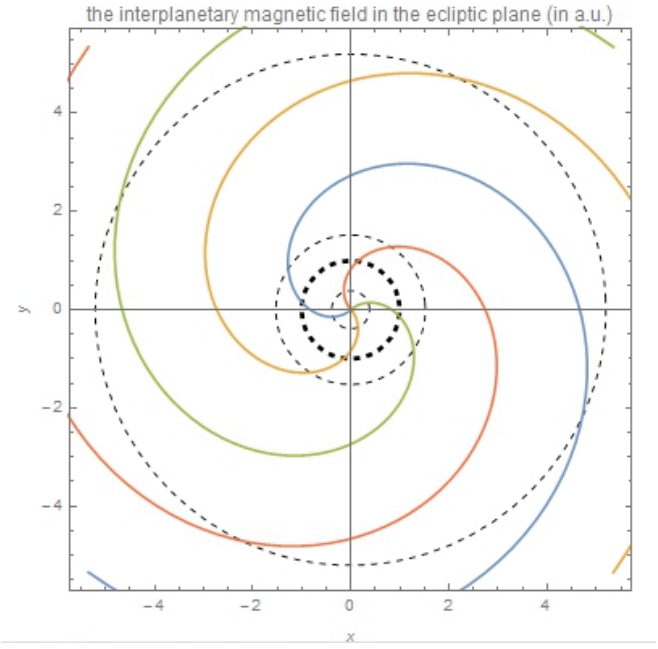

Figure 36 Interplanetary magnetic field (source: Wolfram)

6.7.2 Coronal Hole Winds

Coronal hole and sector reversal winds are the second most common type of solar winds reaching Earth, each occurring 23.9 % of the time from 1995 to 2018.

Coronal hole winds are classified as fast solar winds with speeds of 500 to over 750 km/s (over 1 million miles per hour). Coronal hole winds have the lowest density of the four types of winds with a density of only 3.2 particles per cm^3. Their magnetic field strength is 5.8 nT. The magnetic field orientation of coronal hole winds also tends to be Parker-spiral aligned with large fluctuations about the Parker-spiral direction. In addition, coronal hole winds tend to be somewhat homogeneous in their composition.

The fast winds emanating from coronal holes are referred to as high-speed streams.

Coronal hole winds occur most frequently during the declining phase of the 11 year solar cycle, as shown in Figure 35. Approximately 34% of the solar winds arriving at Earth during the declining phase originate from coronal holes.

High speed solar wind streams originating from coronal holes are a major cause of geomagnetic storms and geomagnetic sub-storms during the solar cycle declining phase. Geomagnetic sub-storms are short duration storms that occur within the polar regions. A major global geomagnetic storm usually has associated with it a number of auroral substorms. However, the reverse is not true. Substorms may appear on their own when there are no mid or low latitude storms. Auroral substorms typically occur at a rate of about 4 per day during the solar cycle declining phase. Auroral borealis sightings are also most prevalent during this phase of the solar cycle.

6.7.3 Sector Reversal Region Winds

Sector reversal winds are blobs of lumpy plasma originating from the stalks of helmet streamers in the vicinity of the heliospheric current sheet. As shown in Figure 31, the current sheet bisects the streamer belt and the helmet streamers located in the region. Pseudostreamers are located far from the heliospheric current sheet and thus do not produce sector reversal winds.

Sector reversal winds, along with coronal hole winds, are the second most common type of solar winds accounting for 23.9 % of the winds reaching Earth from 1995 to 2018. Their speeds range from around 250 to 400 km/s. Consequently, they are classified as very slow solar winds. Sector reversal winds are the densest of the four types of winds with a density of 10.7 particles per cm^3. However, they have the weakest magnetic field strength at 4.3 nT. Sector reversal winds are non-homogeneous with large sudden changes in density, temperature, and magnetic field strength. In addition, the magnetic field orientation of sector reversal winds do not tend to be Parker-spiral aligned.

Solar winds consist primarily of very slow sector reversal winds and slow streamer belt winds during solar minimum. These slow speed winds account in part for the low occurrence of geomagnetic storms and substorms during solar minimum. Typically, one substorm occurs about every 2 or 3 days during solar minimum. In contrast substorms occur at a rate of about 4 per day during the declining phase of the solar cycle when coronal hole winds are most prevalent.

6.7.4 Coronal Mass Ejections Winds

Coronal mass ejection plasma is the fourth type of solar wind.

A coronal mass ejection (CME) is a huge eruption of coronal plasma that moves outward from the Sun into interplanetary space. CMEs vary widely in size, shape, and speed. Some look like loops, others like blobs, and some are irregular in shape. Figure 37 is an example of a CME.

CMEs are often caused by the catastrophic collapse of coronal loops as magnetic fields re-align and reconnect into lower energy states triggering solar flares.

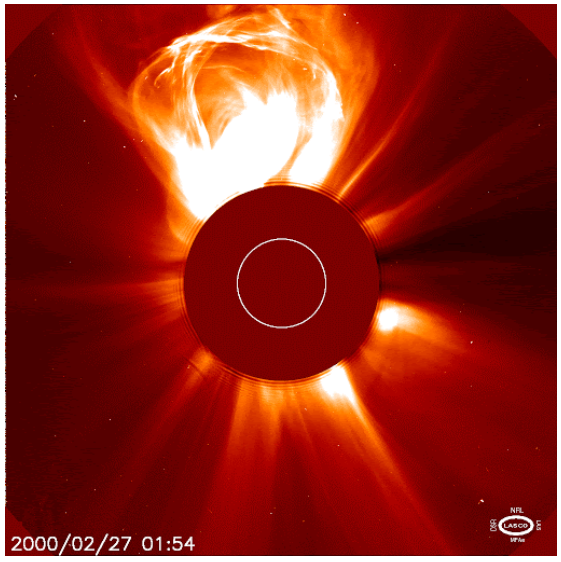

Figure 37 Coronal Mass Ejection (credit: www.astronet.ru)

A CME can eject billions of tons of coronal material outward from the Sun at speeds typically ranging from 200 to 800 km/s. Some energetic CMEs can reach speeds of 3,000 km/s or more.

An interplanetary shock wave is created when a high-speed CME plows through the slower ambient solar wind. The shock wave accelerates charged particles ahead of it. In some cases these particles are accelerated to nearly 80% the speed of light. The small percentage of particles that are accelerated to such high speeds are called solar energetic particles (SEPs). SEPs consist of protons,

electrons and some heavy ions. They are of particular interest because they can damage spacecraft and endanger life in outer space. SEPs originate from both solar flares and CME interplanetary shock waves. However, only about 1% of CMEs produce strong SEP events.

During solar maximum several CMEs of various sizes and shapes occur per day. At solar minimum one CME is typically observed every 5 days or so.

Most CMEs are ejected outward from the Sun into the solar system away from Earth. However, a CME launched in the direction of Earth can arrive in as little as 15-18 hours. Slower CMEs may take several days to arrive. A CME expands as it travels away from the Sun. A large CME can encompass nearly a quarter of the distance between the Sun and Earth by the time it reaches Earth.

A CME is referred to as an Interplanetary Coronal Mass Ejection (ICME) as it moves outward from the Sun into interplanetary space

Coronal mass ejections accounted for 11.5 % of the solar winds reaching Earth from 1995 to 2018. CME winds are the second most dense of the four types of winds with a density of 6.4 particles per cm^3. They also have the strongest magnetic field strength at 10.6 nT. CME winds are non-homogeneous with large sudden changes in density, temperature, and magnetic field strength. In addition, their magnetic field orientation is not Parker-spiral aligned.

Coronal mass ejections are rarely seen during solar minimum. However, they frequently occur around solar maximum becoming a major cause of solar maximum geomagnetic storms. As illustrated in Figure 35, the rate of CMEs steadily decreases during the declining phase of the solar cycle (from solar maximum to solar minimum), but then increase in frequency during the ascending phase of the next cycle.

6.8 Impact of Solar Winds on Earth's Geomagnetic Field

The impact of the 4 types of solar winds on Earth's geomagnetic field is summarized in Table 2. Streamer belt winds are the ambient background solar winds that are present most of the time.

While solar wind speed is a factor, the orientation of the solar wind magnetic field has the greatest impact on the severity of geomagnetic storms, or if storms will occur at all. Geomagnetic storms, including the largest storms, are most likely to develop when the B_Z component of the solar wind magnetic field is directed southward. Relatively few storms develop when the magnetic field is pointed northward.

Solar Cycle Phase	Slow Streamer Belt Winds	Very Slow Sector Reversal Winds	Coronal Mass Ejection Winds	Fast Coronal Hole Winds	Geo-magnetic Storms	Substorms
Minimum	**Ambient continuous background winds**	**High rate of occurrence**	Rare	Average occurrence rate	**Low rate of occurrence**	**1 substorm every 2 – 3 days**
Ascending	Ambient continuous background winds	Average occurrence rate	Average occurrence rate	Low occurrence rate	**Small increase in occurrence**	**Small increase in occurrence**
Maximum	Ambient continuous background winds	Infrequent	**High rate of occurrence**	Average occurrence rate	**Significant increase in occurrence**	**Significant increase in occurrence**
Declining	Ambient continuous background winds	Average occurrence rate	Average occurrence rate	**Very High rate of occurrence**	**High rate of occurrence**	**4 substorms per day**

Table 2 Impact of the various types of solar winds on geomagnetic storms and substorms

Solar Minimum: Solar minimum is the quiet period of the solar cycle with few sun spots and low solar activity. Slow speed streamer belt and sector reversal winds are the dominate solar winds during solar minimum resulting in little geomagnetic activity. Typically, only one substorm occurs every 2 or 3 days.

Ascending Phase: A few coronal mass ejections begin appearing during the ascending phase of the solar cycle resulting in a small increase in geomagnetic activity.

Solar Maximum: Solar maximum is the most active period of the solar cycle with large numbers of sun spots, high levels of EUV and X-ray radiation, and frequent solar flares. Coronal mass ejects occur often during solar maximum resulting in a significant increase in geomagnetic storms and substorms. CME driven geomagnetic storms are the predominate type of magnetic storms during solar maximum.

Declining Phase: Fast coronal hole winds reach their peak during the declining phase of the solar cycle producing large numbers of geomagnetic storms and substorms. Typically, 4 substorms occur each day.

6.9 Corotating Interaction Regions (CIRs)

A Corotating Interaction Region (CIR) is formed when fast solar winds from a coronal hole overtake slow ambient solar winds originating in the streamer belt. The ambient wind on the left in Figure 38 is slowly rotating counterclockwise in a Parker-spiral. The fast wind, also rotating counterclockwise, is plowing through the ambient wind leaving a region of rarefied winds in it wake. A zone of compressed wind, a CIR, develops in front of the high-speed wind as it plows into the slower moving ambient wind. This phenomenon is called corotating because the interaction region rotates along with the coronal hole on the Sun's surface from which the high-speed wind originates. Since coronal holes tend to be long-lived, often persisting for several months, high-speed winds and the resulting CIRs sweep past the Earth at regular intervals corresponding to the 27 day solar rotation period.

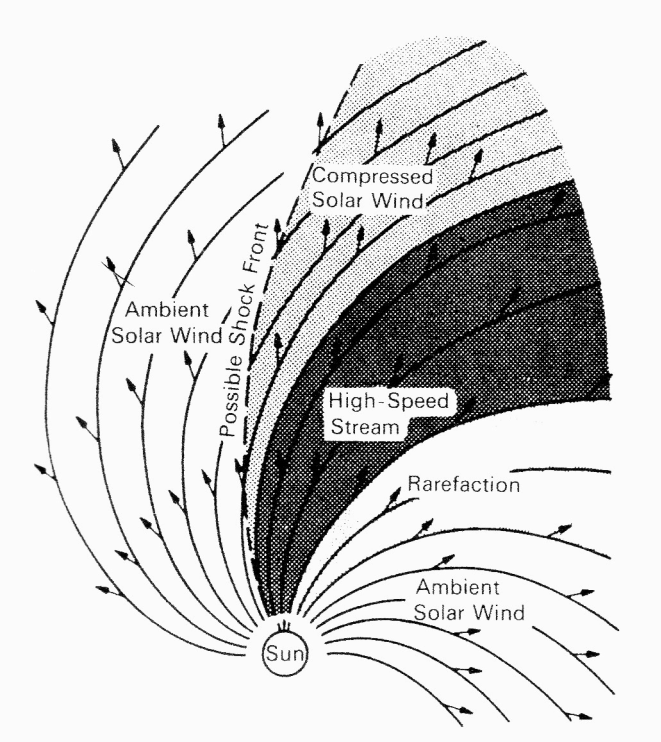

Figure 38 Corotating Interactive Region (source: Hunsucker & Hargreaves)

The section of a corotating interaction region in the vicinity of Earth's orbit is shown in more detail in Figure 39. In this figure the tan area is the CIR zone with the Sun located far below the lower edge of the picture. The unperturbed fast wind from a coronal hole is approaching the CIR from below. Unperturbed slow wind is shown above the CIR. The high-speed wind is slowed down,

compressed and deflected to the right in the lower part of the CIR (indicated by the red arrow) as it crashes into the slower wind ahead of it. The slow wind in turn is sped up, compressed and deflected to the left (red arrow) in the upper part of the CIR. The stream interface (the purple curved line) is the boundary between the fast and slow speed winds.

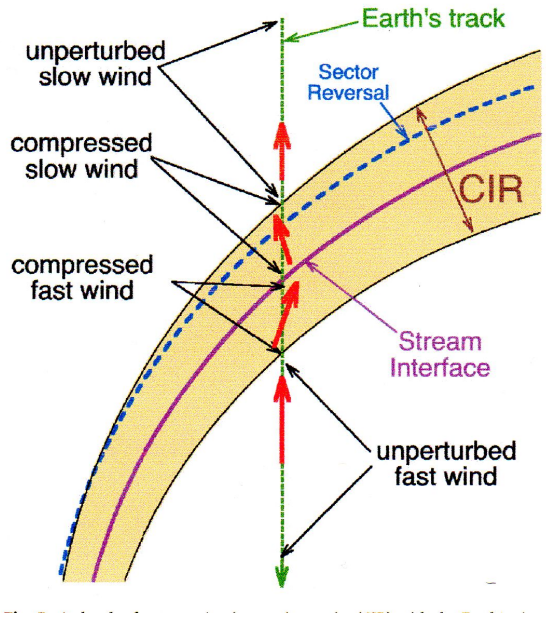

Figure 39 Detailed CIR Diagram (source J. Borovsky)

In Figure 39 the position of the Earth is represented by the green dashed line as the CIR rotates counterclockwise past Earth. Initially the Earth is in the unperturbed slow wind above (in this picture) the CIR. The Earth encounters the compressed slow wind first, followed by compressed fast wind, as the CIR rotates past Earth. After the CIR has passed, the Earth emerges into the unperturbed fast wind below the CIR. It takes about a day for the CIR to pass the Earth. The unperturbed fast wind is often referred to as a high-speed stream (HSS).

Compression within the CIR increases the number density n_{SW} of the solar wind plasma and its magnetic field strength B_{SW}. The elevated density and magnetic field increase the chance of a geomagnetic storm occurring. The CIR will quite likely induce a large storm if the enhanced magnetic field happens to be pointed southward. A northward directed magnetic field will usually not produce a geomagnetic storm. While solar wind speed is a factor, the orientation of the solar wind magnetic field has the greatest impact on the severity of a geomagnetic storm, or if a storm will occur at all.

The unperturbed slow speed wind is associated with either a helmet streamer, containing a sector reversal zone, or a pseudostreamer which does not have a sector reversal. A sector reversal occurs when the radial component of the solar wind magnetic field flips from inward toward the Sun to

outward away from the Sun, or visa versa, as the result of the heilospheric current sheet bisecting a helmet streamer. If a sector reversal zone is present it tends to appear in the CIR a fraction of a day prior to passage of the stream interface. A sector reversal is shown as a blue dashed curved line in Figure 39. The sector reversal, in combination with increased slow speed wind density and magnetic field strength, often represents a calm before the occurrence of a large geomagnetic storm driven by the high-speed wind. The calm often lasts for several days before the on set of the geomagnetic storm. The "calm before the storm" is generally not apparent when the slow speed wind originates from pseudostreamers since they do not have sector reversal zones.

6.10 Earth's Tilt Affect of Geomagnetic Storms

The tilt of the Earth with respect to the Sun varies through out the year resulting in spring, summer, fall, and winter. The Earth's tilt, illustrated in Figure 40, also has an affect on the intensity of geomagnetic storms.

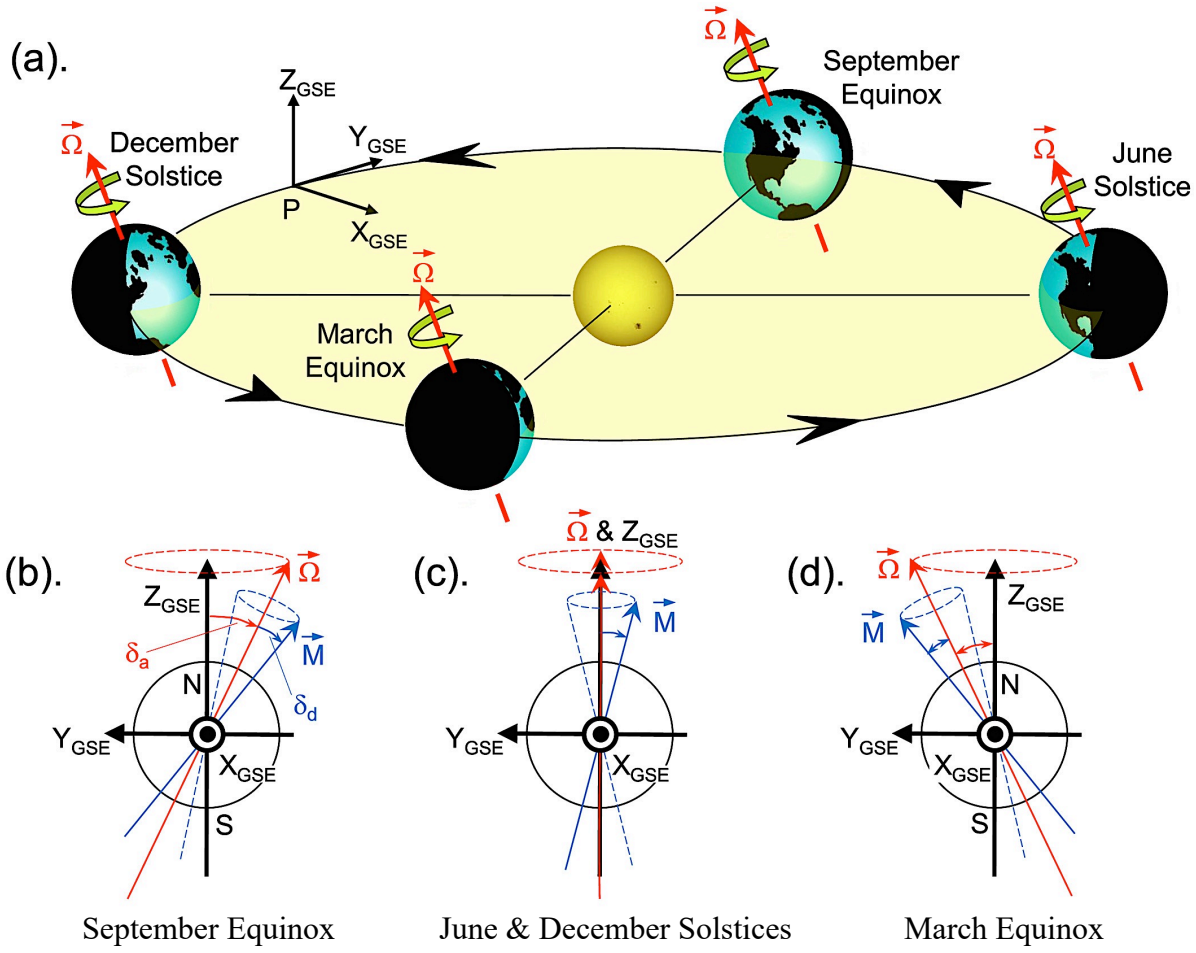

Figure 40 Tilt of the Earth during equinoxes and solstices (source: AGU Publications)

Figure 40a shows the tilt of the Earth at the March Equinox, June Solstice, September Equinox, and December Solstice. The red vector labeled $\vec{\Omega}$ is the Earth's rotational axis. The Geocentric Solar Ecliptic (GSE) coordinate system is shown at point P. The radial X axis (X_{GSE}) is pointed to the Sun. The Y axis (Y_{GSE}) is tangent to Earth's orbit in the ecliptic plane and perpendicular to the radial axis X_{GSE}. Finally, the Z axis (Z_{GSE}) is perpendicular to the ecliptic plane. Figures 40 b, c, and d shows the tilt of Earth's rotational axis (red arrow) and magnetic axis (blue arrow) at significant times of the year.

The angle of Earth's rotational axis relative to the Z_{GSE} axis is always 23.4^o . The Earth's axis gyrates around Z_{GSE} throughout the year as shown in Figures 40 b, c, and d. At the December Solstice Earth's axis is pointed away from the Sun in the negative X_{GSE} direction. In June the Earth's axis is pointed in the positive X_{GSE} direction toward the Sun creating long summer days in the northern hemisphere. The solstices are the only times of the year when the Y_{GSE} component of Earth's tilt is zero. The June and December Solstices are shown in Figure 40c. During the March Equinox Earth's axis is pointed in the positive Y_{GSE} direction, as shown in Figure 40d, while its X_{GSE} component is zero. During the September Equinox Earth's axis is titled in the negative Y_{GSE} direction, as shown in Figure 40b, again with a zero X_{GSE} component. At other times of the year (other than the equinoxes) the X_{GSE} component of Earth's tilt is non-zero.

In spring and fall the Y_{GSE} tilt of Earth is such that Earth's magnetic field is more closely aligned with that of the Parker-spiral magnetic field orientation of the unperturbed high-speed winds. If the high-speed wind magnetic field is directed southward (in the $-Z_{GSE}$ direction) it will connect with Earth's favorably aligned magnetic field creating geomagnetic storms that are more intense than at other times of the year. The unperturbed fast winds emanating from coronal holes can persist for several days or longer, so high-speed wind driven geomagnetic storms can persist for a long time. However, few if any geomagnetic storms will occur if the high-speed wind magnetic field happens to be directed northward. During the summer and winter Earth's tilt results in less favorable alignment with high-speed wind magnetic fields resulting less severe geomagnetic storms. These ideas were suggested by Russell and McPherron in 1973.

6.11 Heliosphere

The heliosphere, Figure 41, is a vast bubble like region of space that surrounds the solar system. It extends out more than 100 AU from the Sun (Figure 42), far past the orbit of Pluto.

The heliosphere is formed by the solar winds emanating from the Sun. The solar winds thin as they travel outward. At around 100 AU the decreasing outward pressure (away from the Sun) exerted by the solar winds becomes equal to the inward pressure of interstellar wind. This region is known as the heliopause. The heliopause marks the outer edge of the heliosphere and the beginning of interstellar space.

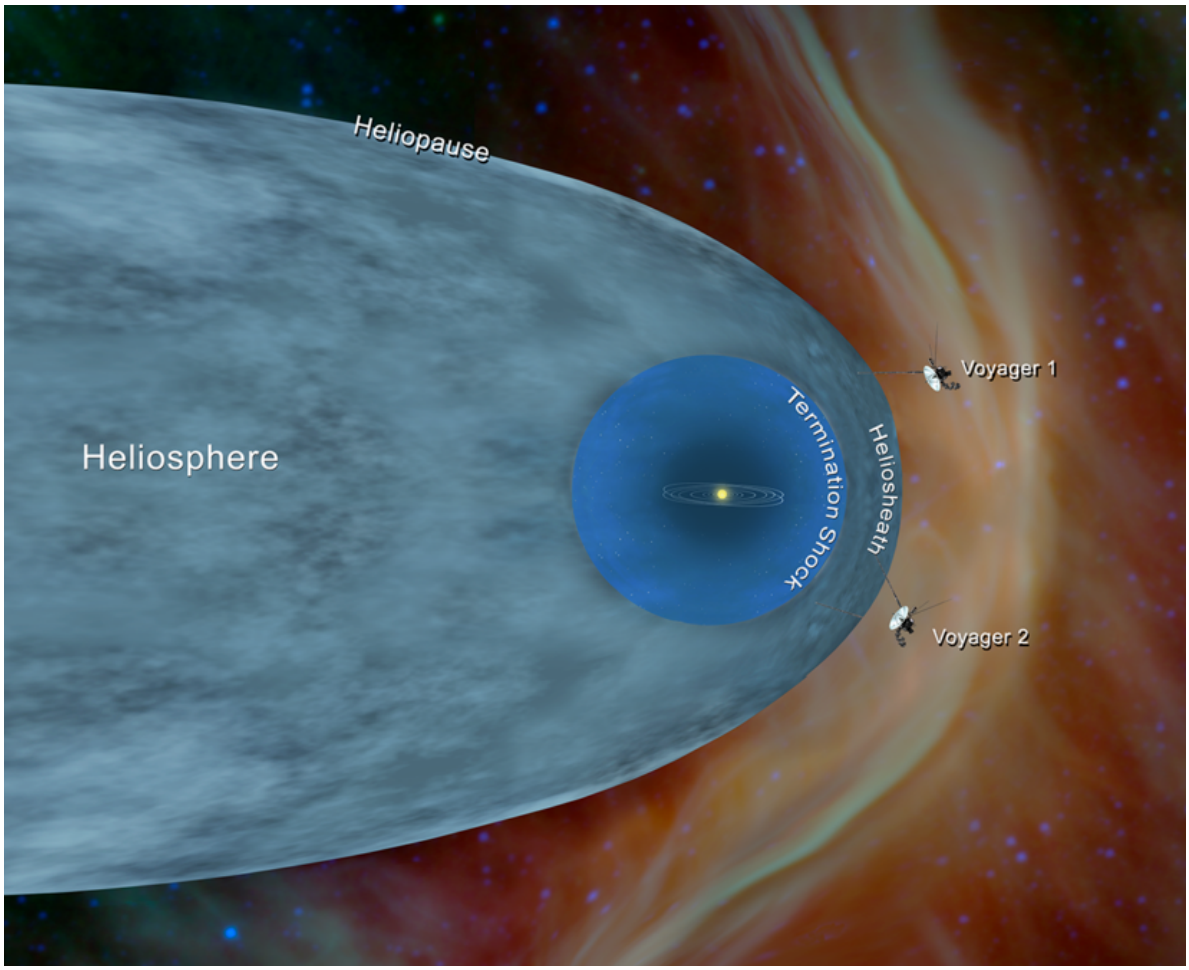

Figure 41 Heliosphere (source: JPL)

Interstellar wind is predominately created by the motion of the solar system as it travels through the interstellar medium (ISM) which sparsely fills the space between the stars and galaxies. The extremely tenuous interstellar medium consists primarily of hydrogen (91%), helium (8.9%), and trace amounts of carbon, oxygen, and nitrogen in rarified ionic, atomic and molecular states. The solar system travels through the ISM at a speed of roughly 220 km/s in its orbit around the center of our galaxy. It is interesting to note that it takes the solar system about two hundred and fifty million (250,000,000) years to orbit the galaxy once.

The speed at which the solar system is traveling through the ISM distorts the heliosphere causing it to have a comet like shape with a blunt nose and a tail stretching out far behind, as shown in Figure 41. This shape is in contrast to the spherical shape that one would expect from solar wind flowing radially out from the Sun. The comet like shape is the result of the ISM wind bending the solar wind back toward the heliospheric tail as illustrated in Figure 41.

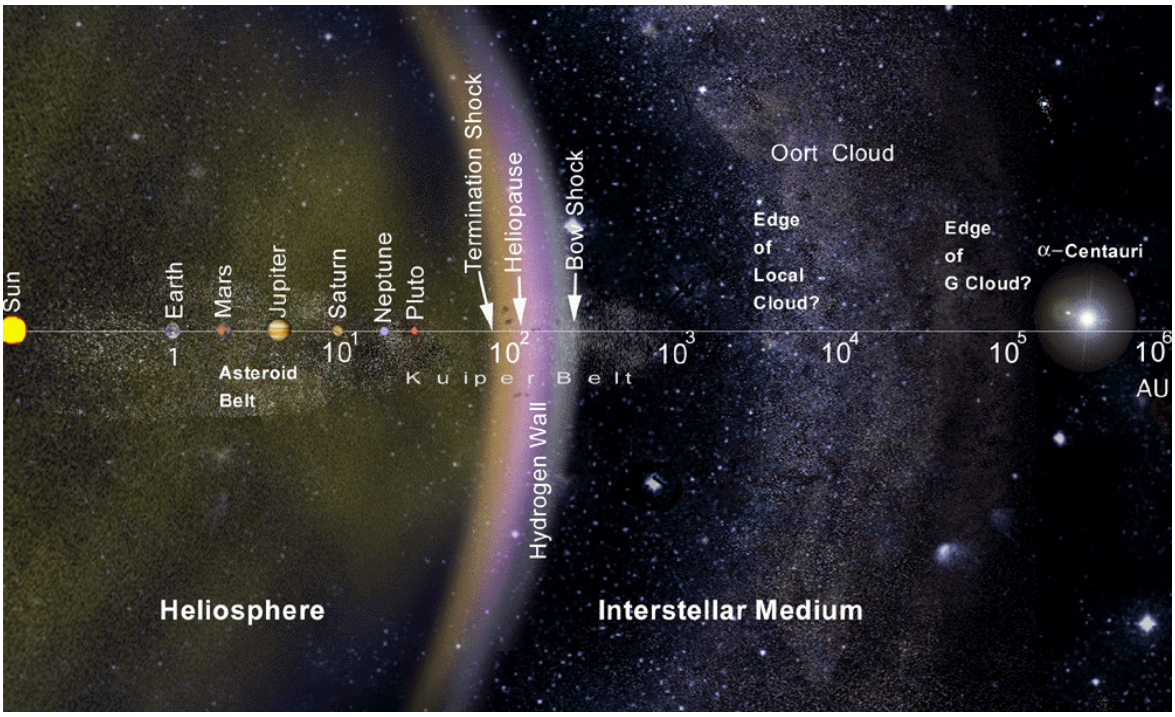

Figure 42 Heliosphere and Interstellar Medium (source: Wikipedia)

The structure of the heliosphere is shown in Figure 43.

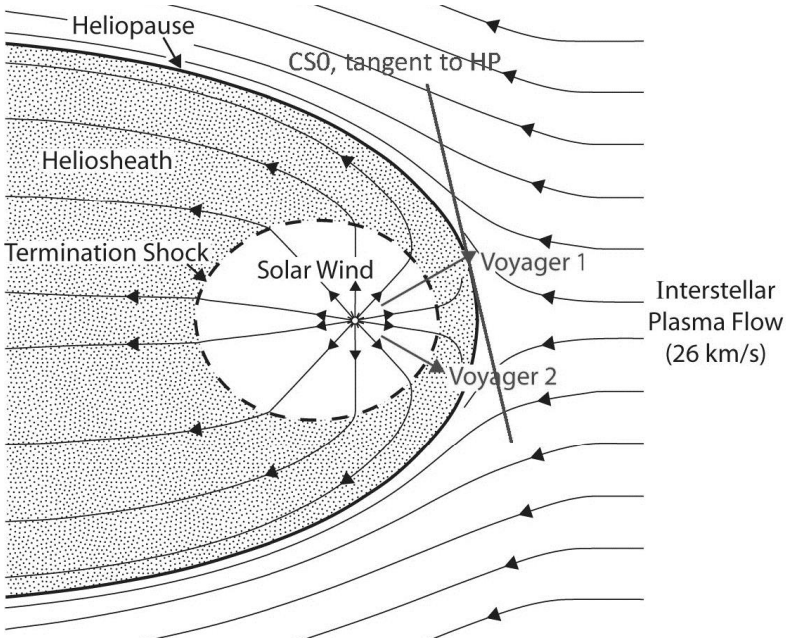

Figure 43 Structure of the heliosphere (source: Wikipedia)

The heliosphere consists of 4 basic regions:

- The **Inner Heliosphere** is the location of Sun and the planets.

- The **Termination Shock** is the region where the supersonic 300 to 800 km/s solar wind abruptly drops below the speed of sound (becomes subsonic) as it begins to feel the effects of the interstellar wind. The speed of sound is the speed at which pressure waves travel through the solar wind plasma. The speed of sound depends on the density of the medium through which it is traveling. For the solar wind plasma, the speed of sound is around 100 km/s.

- The **Heliosheath** is the broad transitional region of the heliosphere between the termination shock and the heliopause. The solar wind continues to flow outward in the heliosheath, but becomes denser and hotter as it piles up against the approaching interstellar wind.

- The **Heliopause** is the outer edge of the heliosphere. It is the boundary between the solar wind and the interstellar wind where the pressure of the two winds is equal but opposite in direction.

The outward pressure of the solar wind varies far more rapidly than the inward pressure of the ISM. Consequently, the location of the terminal shock and heliopause are continually moving inward and outward as the solar wind changes, including changes resulting from the roughly 11 year solar cycle.

Voyager 1 has left the solar system crossing the heliopause on August 25, 2012. Voyager 2, following a different route, left the solar system crossing the heliopause on November 5, 2018. Notice the positions of Voyagers 1 and 2 in Figure 41. Both spacecraft are now traveling through interplanetary space. The Voyagers have enough electrical power and thruster fuel to keep operating until at least 2025. Once they fall silent, they will likely wander eternally through the Milky Way Galaxy.

References

Khazanov, George V.; "Space Weather Fundamentals"; CRC Press, 2016

Foukal, Peter; "Solar Astrophysics third edition"; Whiley-VCH Publishing Company, 2013

Hunsucker R. D.; Hargreaves, J. K.; "The High-Latitude Ionosphere and its Effects on Radio Prdopagation"; Cambridge University Press 2003

Davies, Kenneth; "Ionospheric Radio"; Peter Peregrinus Ltd.,1990

McNamara, Leo F.; "The Ionosphere: Communications, Surveillance, and Direction Finding"; Krieger Publishing Company, 1991

Carroll, Bradley W. and Ostlie, Dale A.; "An Introduction to Modern Astrophysics"; Addison-Wesley Publishing Company Inc., 1996

Golub, Leon and Pasachoff, Jay M.; "Nearest Star The Surprising Science of Our Sun second edition"; Cambridge University Press, 2014

Moldwin, Mark; "An Introduction to Space Weather"; Cambridge University Press, 2008

Goodman, John M.; "Space Weather & Telecommunications"; Springer Science+Business Media Inc. 2005

Cander, Ljiljana R.; "Ionospheric Space Weather"; Springer Nature Switzerland AG 2019

Borovshy, Joseph E.; "What magnetospheric and ionospheric researchers should know about the solar wind"; Space Science Institute, Boulder, CO.

Xu, Fei; Borovsky, Joseph E.; "A new four plasma categorization scheme for the solar wind"; 15 December 2014, https://doi.org/10.1002/2014JA02412

Russell, C. T.; McPherron, R. L.; "Semiannual Variation of Geomagnetic Activity"; Journal of Geophysical Research Vol. 78, No. 1 January 1, 1973

Zhao, Hong and Zong, Q.G.; "Seasonal and diurnal variation of geomagnetic activity: Russell-McPherron effect during different IMF polarity and/or extreme solar wind conditions" ; Journal of Geophysical Research Atmospheres, November 2012

Richardson, Ivan G.; "Solar wind stream interaction regions throughout the heliosphere"; NASA Goddard Space Flight Center, Greenbelt, MD, January 26, 2018

Mathew, Mike Lockwood et al; "On the origins and timescales of geoeffective IMF"; 02 June 2016 https://doi.org/10.1002/2016SW001375

McPherron, Robert L.; Weygand, James; "The Solar Wind and Geomagnetic Activity as a Function of Time Relative to Corotating Interaction Regions"; Institute of Geophysics and Planetary Physics and Department of Earth and Space Science University of California, Los Angeles, California. USA

Alves, M. V.; Echer, E.; Gonzalez, W. D.; "Geoeffectiveness of corotating interaction regions as measured by Dst index"; 12 May 2006 https://doi.org/10.1029/2005JA011379

Axford,W. I.; Suess, S.T.; "The Heliosphere"; Max-Planck – Institut fur Aeronomie Postfach 20, Katlenburg-Lindau, D 3411 Germany; Space Science Lab/ES82 NASA Marshall Space Flight Center Huntsville, Alabama, USA

Luhmann, J. G.; "Living With The Sun"; Space Sciences Lab, University of California, Berkeley

Saez, F.; Zhukov, A. N.; Lamy, P.; and Llebaria, A.; "On the 3-dimensional structure of the streamer belt of the solar corona; Astronomy & Astrophysics

Friedman, Herbert; "The Astronomer's Universe Stars, Galaxies, and Cosmos"; W. W. Norton & Company, 1990

Piccioni, Robert L.; Everyone's guide to Atoms Einstein and the Universe second edition"; Real Science Publishing, 2010

Hogan, Craig J.; "The Little Book of the Big Bang A Cosmic Primer"; Springer-Verlag New York, Inc., 1998

Zirin, Harold and Lang, Kenneth; "Sun - Astronomy"; Encyclopedia Britannica

Kuznetsov, V. D.; "From the geophysical to heliophysical year: The results of the CORONAS-F project"; Russian Journal of Earth Sciences, Vol. 9, ES3004, doi: 10.2205/2007ES000276, 2007

Hathaway, David H., Wilson, Robert M., Reichmann, Edwin J.; "Group Sunspot Numbers: Sunspot Cycle Characteristics"; NASA/Marshall Space Flight Center, Huntsville, AL., 2002

Minzner, R. A.; "The 1976 Standard Atmosphere Above 86 km Altitude" NASA Goddard Space Flight Center, 1976

Masi, Marco; "Quantum Physics: an overview of a weird world"; Marco Masi 2018

Zettili, Nouredine; "Quantum Mechanics Concepts and Applications second edition"; John Wiley & Sons, 2009

Ahrens, C. Donald; "Essentials of Meteorology"; Wadsworth Publishing Company, 1998

Halliday, David and Resnick, Robert; "Physics For Students of Science and Engineering Part II second edition"; John Wiley & Sons, Inc., 1962

Zumdahl, Steven S. “Chemistry second edition”; D. C. Heath and Company, 1989

Dr. David Hathaway, Dr. Lisa Upton "Solar Cycle Science Discover the Sun!"
http://solarcyclescience.com/